Supplementary Information (SI) for Inorganic Chemistry Frontiers.

Supporting Information

Unsupported gallatabenzene via rare-earth-metal pentadienyl complexes

Jakob Lebon,[a] Manfred Manßen,[a] Cäcilia Maichle-Mössmer,[a] Peter Sirsch*[a] and Reiner Anwander*[a]

Institut für Anorganische Chemie, Eberhard Karls Universität Tübingen, Auf der Morgenstelle 18, 72076 Tübingen, Germany

*E-mail for R.A.: reiner.anwander@uni-tuebingen.de

Table of Contents

Experimental Section

General Considerations. All manipulations were performed under rigorous exclusion of air and moisture using standard Schlenk, high-vacuum, and glovebox techniques (MBraun UNIlab pro ECO); <0.5 ppm O_2, <0.5 ppm H_2O, argon atmosphere). *n*-Hexane, toluene and THF were purified using Grubbs Columns (MBraun SPS, solvent purification system), THF was further dried over molecular sieves (3 Å). Benzene was dried over CaH_2 and distilled onto molecular sieves (3 Å). C_6D_6 (99.6%, Sigma-Aldrich), toluene-d_8 (99.6%, Sigma-Aldrich) and thf-d_8 (Sigma-Aldrich) were dried by letting the solvents stand over Na/K-alloy for at least 24 h and subsequent filtration. All solvents were stored inside a glovebox. Compounds (C_5Me_5)Y(μ-Me)(AlC_5H_3Me-1-*t*Bu_2-3,5) (**1**) and (1-Me-3,5-*t*Bu_2-C_5H_3Ga)(μ-Me)Y(1-Me-3,5-*t*Bu_2-C_5H_3Ga) (**4**) were synthesized according to literature procedures.[1,2] Tetramethylsilane (TMS) was purchased from Sigma-Aldrich and distilled, and stored in a glovebox prior to use. NMR spectra of air and moisture sensitive compounds were recorded by using J. Young valve NMR tubes at ambient temperature on either a Bruker AVII+400 (^{1}H, ^{13}C), a Bruker DRX-300 or a Bruker AVII+500. NMR chemical shifts are referenced to internal solvent resonances and reported in parts per million relative to TMS. Coupling constants are given in Hertz. Elemental analyses were performed on an Elemental Vario Micro Cube.

(1-Me-3,5-*t*Bu_2-C_5H_3Al)(μ-AlMe_4)Y(C_5Me_5) (2).

To a solution of 100 mg of complex **1** (1 equiv., 0.218 mmol) dissolved in *n*-hexane a solution of 15.72 mg $AlMe_3$ (1 equiv., 0.218 mmol) in *n*-hexane was added. The reaction mixture was stirred for 24 h at ambient temperature. Then, TMS was added to the orange-yellow solution and stored at –40 °C to form crystals. Compound **2** was obtained as an orange solid in 66% yield. The yield was taken after the solution over the crystals was pipetted off and the remaining solvent evaporated at ambient temperature and pressure.

[(1-Me-3,5-*t*Bu_2-C_5H_3Al)(thf)(3,5-*t*Bu_2-C_5H_3(Al-Me_2)][3).

To a solution of 200 mg of complex **1** (2 equiv., 0.396 mmol) dissolved in thf/toluene a slurry of $AlCl_3$ (1 equiv., 0.198 mmol) in thf/toluene was added. The reaction mixture was stirred for 24 h at ambient temperature. Aliphatic phases derived therefrom were concentrated in vacuo and the reddish precipitate was extracted with *n*-pentane and TMS to achieve an orange solution which formed crystals at –40 °C. Compound **3** was obtained as an orange solid in 66% yield. ^{1}H NMR, (500 MHz, C_6D_6, 8 °C): δ 6.21 (s, Hz, 2H, –C*H*=), 4.31 (dd, $^4J_{H,H}$ = 2.0 Hz, 1H, –C*H*=), 4.29 (s, 2H, –C*H*=), 3.42 (s, 1H, –C*H*=), 3.15 (s, 4H, thf), 1.45 (s, 9H, C(CH_3)$_3$), 1.34 (s, 9H, C(CH_3)$_3$), 1.24 (s, 9H, C(CH_3)$_3$), 0.92 (s, 4H, thf), -0.18 (s, 3H, Al–CH_3), -0.21 (s, 6H, Al–CH_3) ppm. ^{13}C{^{1}H} NMR (126 MHz, C_6D_6, 8 °C): δ 197.9 (s, 2C, –*C*CMe$_3$), 197.3 (s, 1C, –*C*CMe$_3$), 195.1 (s, 1C, –*C*CMe$_3$), 112.1 (s, 1C, –*C*H=), 106.1 (s, 1C, –*C*H=), 77.5 (s, 1C, –*C*H=), 73.6 (s, 2C, –*C*H=), 70.1 (s, 2C, –*C*H–$_{(thf)}$), 65.8 (s, 1C, –*C*H=), 41.7 (s, 4C, –*C*(CH$_3$)$_3$), 31.0 (s, 12C, –C(*C*H$_3$)$_3$), 25.3 (s, 2C, –*C*H–O$_{(thf)}$), -5.7 (s, 1C, –Al–*C*H$_3$), -11.6 (s, 2C, –Al–*C*H$_3$) ppm. Elemental analysis: $C_{33}H_{59}Al_3O$ (522.78 g/mol): C 71.70%, H 10.76%; found: C 70.98%, H 10.62%.

[(1-Me-3,5-*t*Bu$_2$-C$_5$H$_3$Ga)(3,5-*t*Bu$_2$-C$_5$H$_3$(Ga-Me)$_2$)] (5).

To a solution of 200 mg of complex **4** (1 equiv., 0.280 mmol) dissolved in *n*-hexane a slurry of $GaCl_3$ (1 equiv., 0.280 mmol) in *n*-hexane was added. The reaction mixture was stirred for 24 h an ambient temperature. The slurry was concentrated in vacuo and the reddish precipitate was extracted with *n*-pentane and TMS to achieve an orange solution which formed crystals at –40 °C. Compound **5** was obtained as an orange solid in 87% yield. ^{1}H NMR, (500 MHz, toluene-d$_8$, –20 °C): *δ* 6.53 (s, 1H, –C*H*=), 6.22 (s, 1H, –C*H*=), 5.09 (s, 2H, –C*H*=), 4.23 (s, 2H, –C*H*=), 2.82 (s, 1H, –C*H*=), 1.26 (s, 18H, C(C*H*$_3$)$_3$), 1.20 (s, 9H, C(C*H*$_3$)$_3$), 1.16 (s, 9H, C(C*H*$_3$)$_3$), 0.13 (s, 3H, Ga–C*H*$_3$), -0.06 (s, 6H, Ga–C*H*$_3$) ppm. ^{13}C{^{1}H} NMR (126 MHz, toluene-d$_8$, –20 °C): *δ* 200.0 (s, 2C, –*C*CMe$_3$), 199.3 (s, 1C, –*C*CMe$_3$), 188.1 (s, 1C, –*C*CMe$_3$), 113.1 (s, 1C, –*C*H=), 109.3 (s, 1C, –*C*H=), 82.3 (s, 2C, Ga–*C*H=), 81.8 (s, 1C, –*C*H=), 57.8 (s, Hz, 1H, Ga–C*H*=), 41.0 (s, 2C, –*C*(CH$_3$)$_3$), 40.2 (s, 1C, –*C*(CH$_3$)$_3$), 40.1 (s, 1C, –*C*(CH$_3$)$_3$), 30.5 (s, 6C, –C(*C*H$_3$)$_3$), 30.4 (s, 3C, –C(*C*H$_3$)$_3$)), 30.1 (s, 3C, –C(*C*H$_3$)$_3$), -0.9 (s, 1C, –Ga–*C*H$_3$), -8.0 (s, 2C, –Ga–*C*H$_3$) ppm. Elemental analysis: $C_{29}H_{51}Ga_3$ (608.85 g/mol): C 57.21%, H 8.44%; found: C 58.01%, H 11.82%. The hydrogen result is outside the range of analytical purity, but no better elemental analysis could be obtained to date.

[(1-Me-3,5-*t*Bu$_2$C$_5$H$_3$GaMe)(*μ*-K)(thf)]$_n$ (6).

To a solution of 200 mg of complex **4** (1 equiv., 0.280 mmol) in *n*-hexane a slurry of KO*t*Bu (2 equiv., 0.560 mmol) in *n*-hexane was added. The reaction mixture was stirred for 24 h at ambient temperature, after addition of one drop thf. The slurry was concentrated in vacuo and extracted with *n*-pentane, filtered and stored at -40 °C. Complex **6** was obtained as colorless crystals (needles) in a yield of 68%. ^{1}H NMR, (500 MHz, thf-d$_8$, 26 °C): *δ* 6.63 (s, $^4J_{H,H}$ = 1.63 Hz, 2H, Ga–C*H*=C), 5.74 (t, $^4J_{H,H}$ = 1.98 Hz, 1H, –C*H*–), 1.27 (s, 18H, C(C*H*$_3$)$_3$), -0.09 (s, 3H, Ga–C*H*$_3$) ppm. ^{13}C{^{1}H} NMR (126 MHz, thf-d$_8$, 26 °C.): *δ* 161.7 (s, 2C, –*C*CMe$_3$), 121.2 (s, 1C, C–*C*H–C), 97.0 (s, 2C, Ga–*C*H=), 39.3 (s, 2C, C*C*Me$_3$), 33.2 (s, 6C, C(*C*H$_3$)$_3$), -9.8 (s, 1C, Ga–*C*H$_3$) ppm. Elemental analysis: $C_{18}H_{32}GaKO$ (373.27 g/mol): C 57.92%, H 8.64%; found: C 55.76%, H 9.01%. The carbon result is outside the range of analytical purity, but no better elemental analysis could be obtained to date.

[(1-Me-3,5-*t*Bu$_2$C$_5$H$_3$GaMe)][K(2.2.2-crypt)] (7).

To a solution of 100 mg of complex **6** (0.267 mmol) in Et_2O a solution of 100.86 mg [2.2.2]-cryptand in Et_2O was added and stirred at ambient temperatures for 1 h. The mixture was concentrated in vacuo and stored at -40 °C. Complex **7** was obtained as pale-yellow crystals in a yield of 85%. ^{1}H NMR, (400 MHz, thf-d$_8$, 26 °C): *δ* 6.41 (s, $^4J_{H,H}$ = 1.7 Hz, 2H, Ga–C*H*=C), 5.57 (t, 1H, $^3J_{H,H}$ = 1.95 Hz, –C*H*–), 3.50 (s, 12H, –O(C*H*$_2$)$_2$O–), 3.48–3.45 (t, $^2J_{H,H}$ = 4.63 Hz, 12H, –N(CH$_2$)(C*H*$_2$)O), 2.50–2.47 (t, 12H, $^2J_{H,H}$ = 4.61 Hz, –N(C*H*$_2$)(CH$_2$)O), 1.24 (s, 18H, C(C*H*$_3$)$_3$), -0.16 (s, 3H, Ga–C*H*$_3$) ppm. ^{13}C{^{1}H} NMR (101 MHz, thf-d$_8$, 26 °C.): *δ* 159.0 (s, 2C, –*C*CMe$_3$), 119.7 (s, 1C, C–*C*H–C), 97.2 (s, 2C, Ga–*C*H=), 71.4 (s, 6C, –O(*C*H$_2$)$_2$O–), 68.5 (s, 6C, –N(CH$_2$)(*C*H$_2$)O), 54.8 (s, 6C, –N(*C*H$_2$)(CH$_2$)O), 39.0 (s, 2C, C*C*Me$_3$), 33.9 (s, 6C, C(*C*H$_3$)$_3$), -8.5 (s, 1C, Ga–*C*H$_3$) ppm. Elemental analysis: $C_{32}H_{60}GaKN_2O_6$ (677.66 g/mol): C 56.72%, H 8.92%, N 4.13%; found: C 56.25%, H 9.07%, N 4.53%.

NMR Spectra

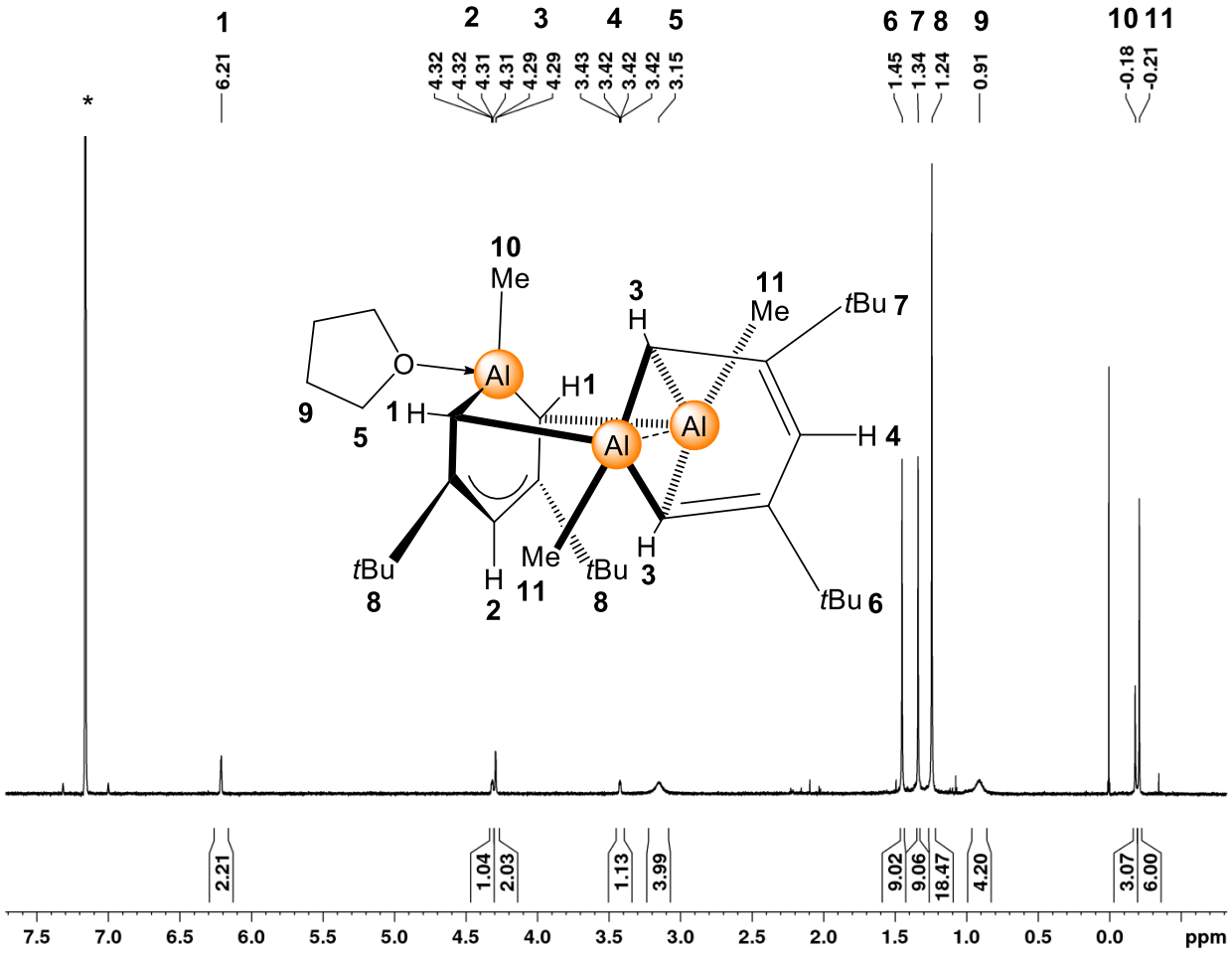

Figure S1. ^{1}H-NMR spectrum (500 MHz) of **3** in C_6D_6 at 8 °C. The solvent residual signal is marked with an asterisk.

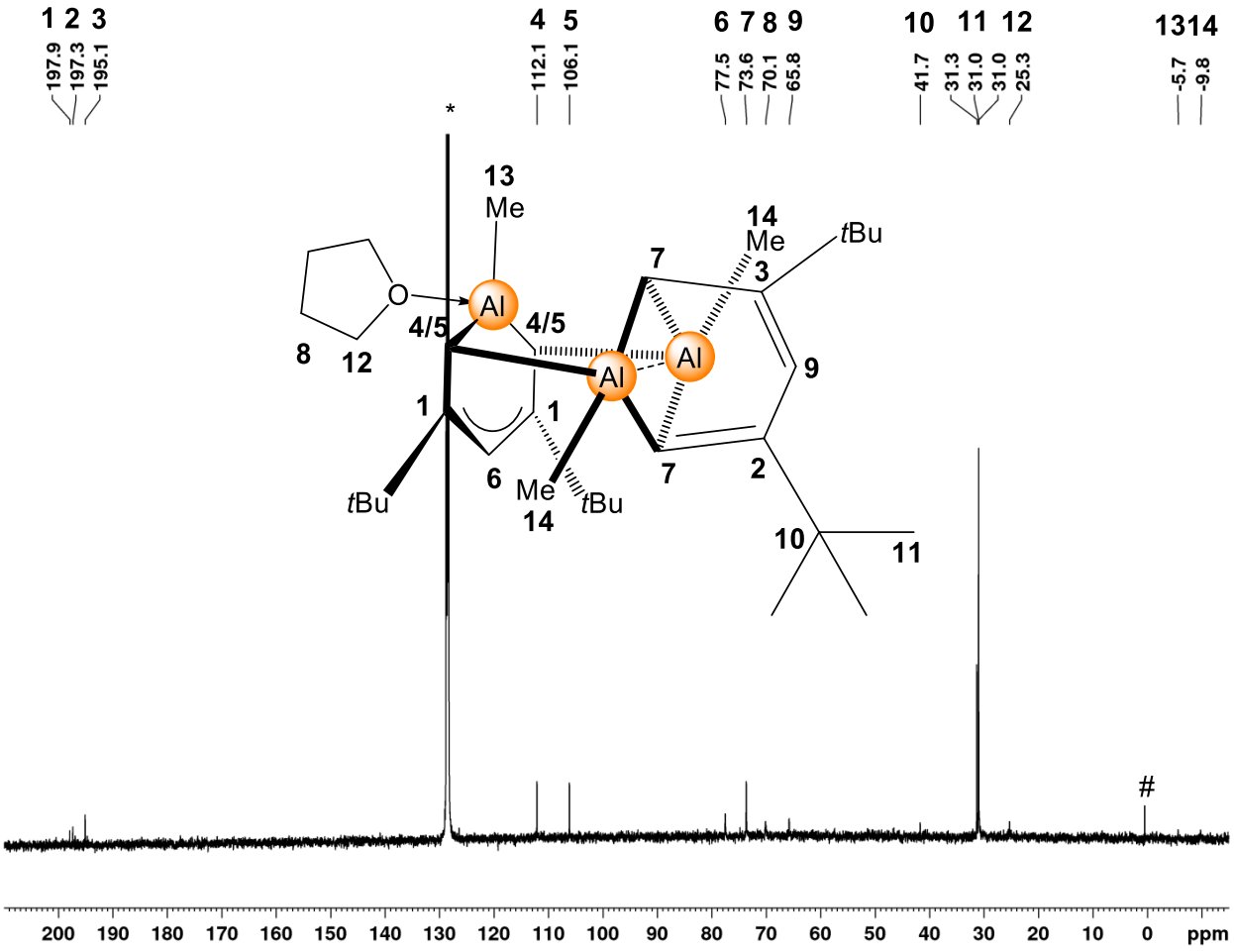

Figure S2. $^{13}C\{^{1}H\}$-NMR spectrum (126 MHz) of **3** in C_6D_6 at 8 °C. The solvent residual signal is marked with an asterisk, impurities with #.

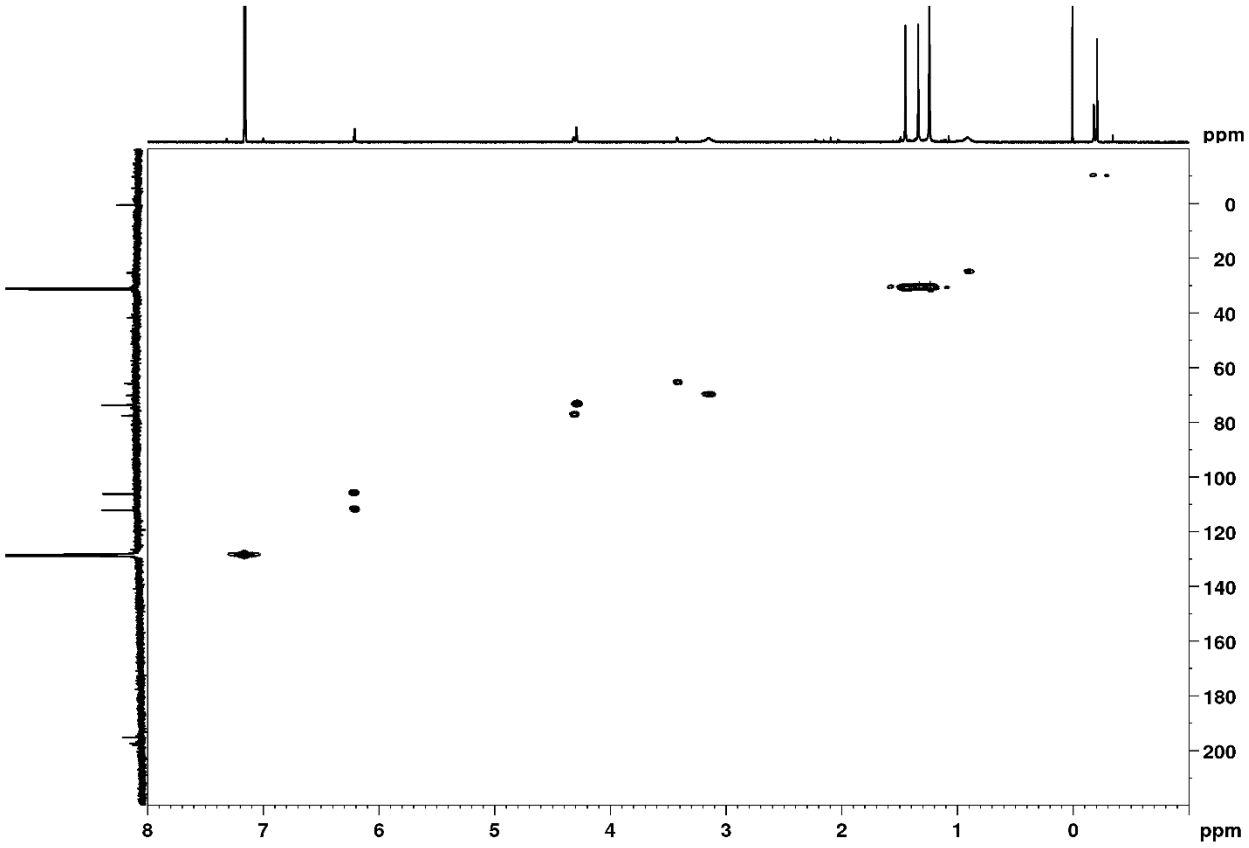

Figure S3. ^{1}H-^{13}C HSQC spectrum (126 MHz) of **3** in C_6D_6 at 8 °C.

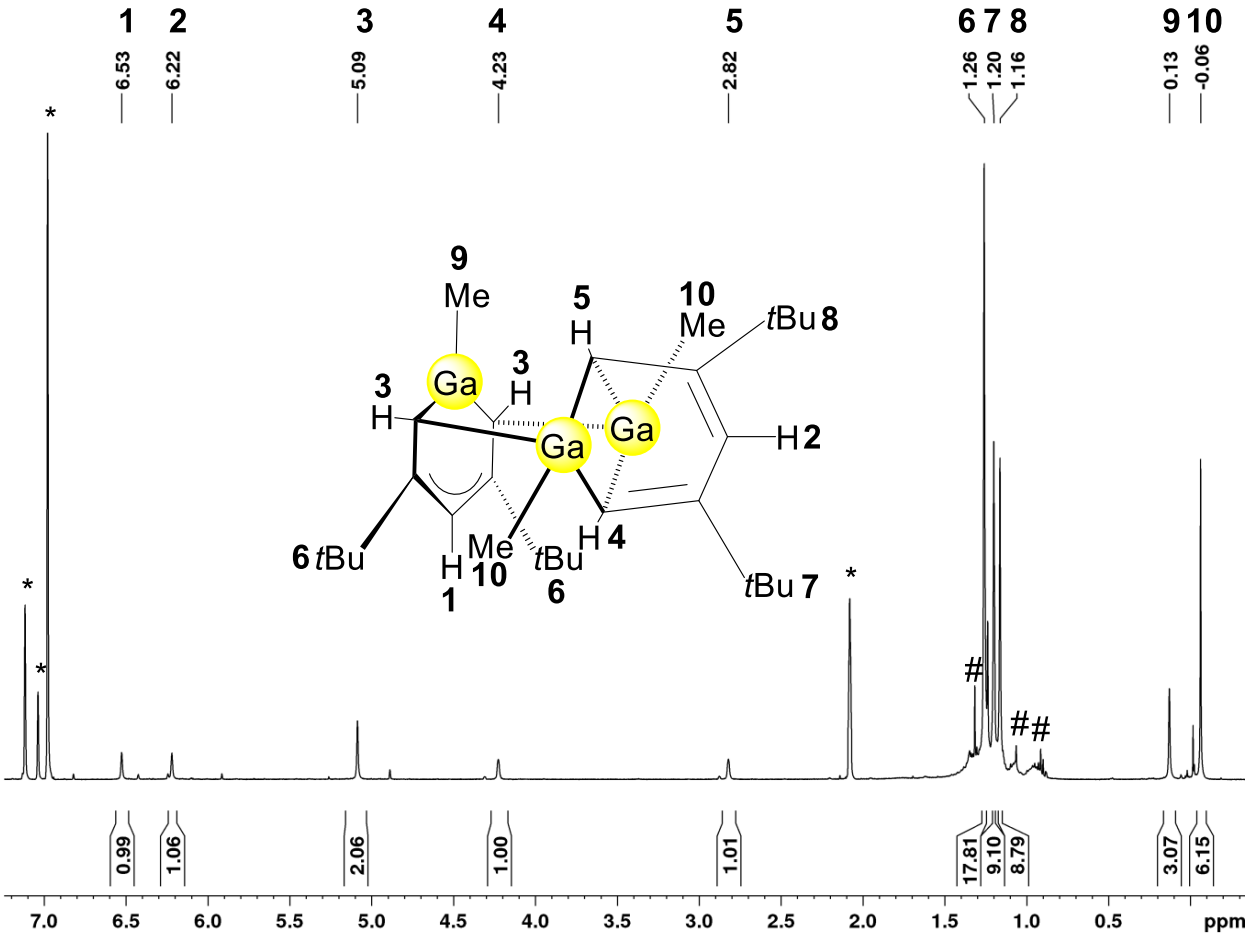

Figure S4. ^{1}H-NMR spectrum (500 MHz) of **5** in toluene-d_8 at –20 °C. The solvent residual signal is marked with an asterisk, impurities with #.

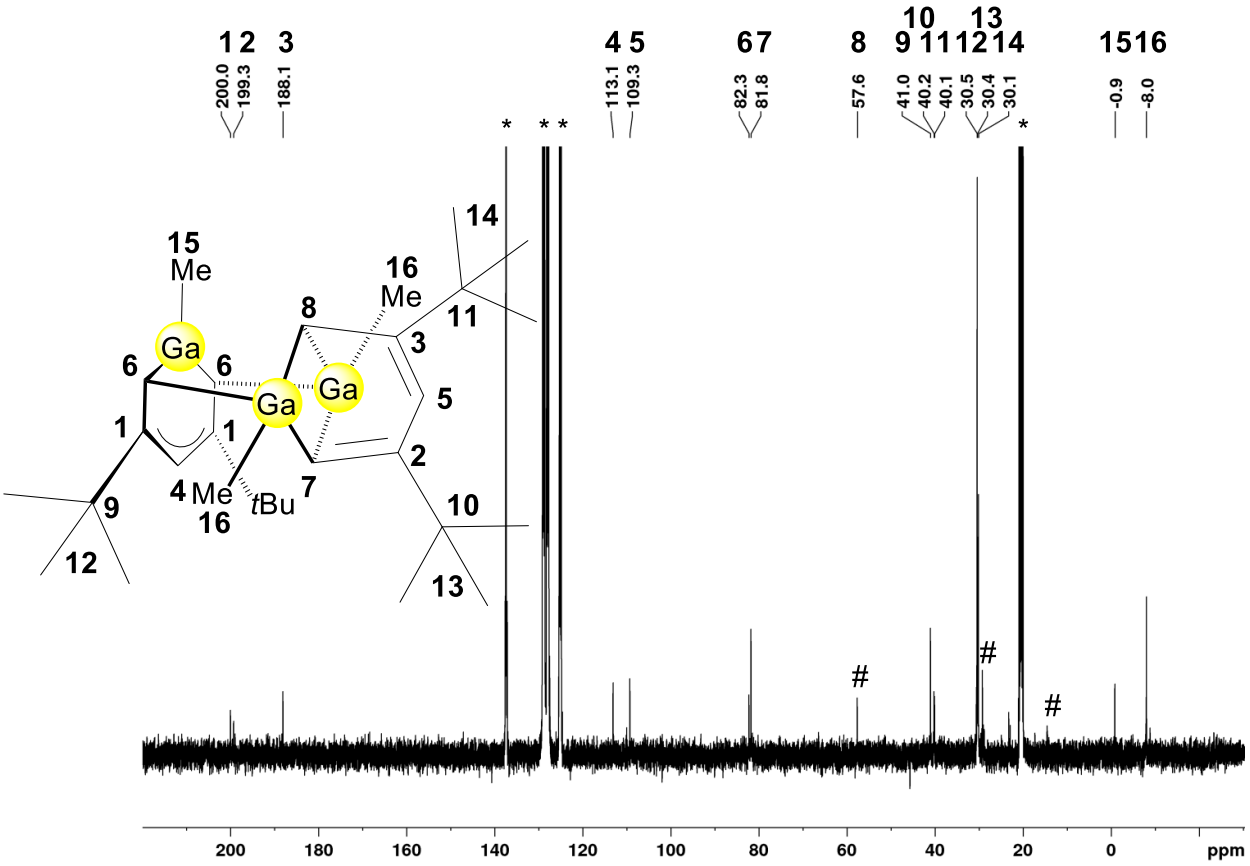

Figure S5. $^{13}C\{^{1}H\}$-NMR spectrum (126 MHz) of **5** in toluene-d_8 at –20 °C. The solvent residual signal is marked with an asterisk, impurities with #.

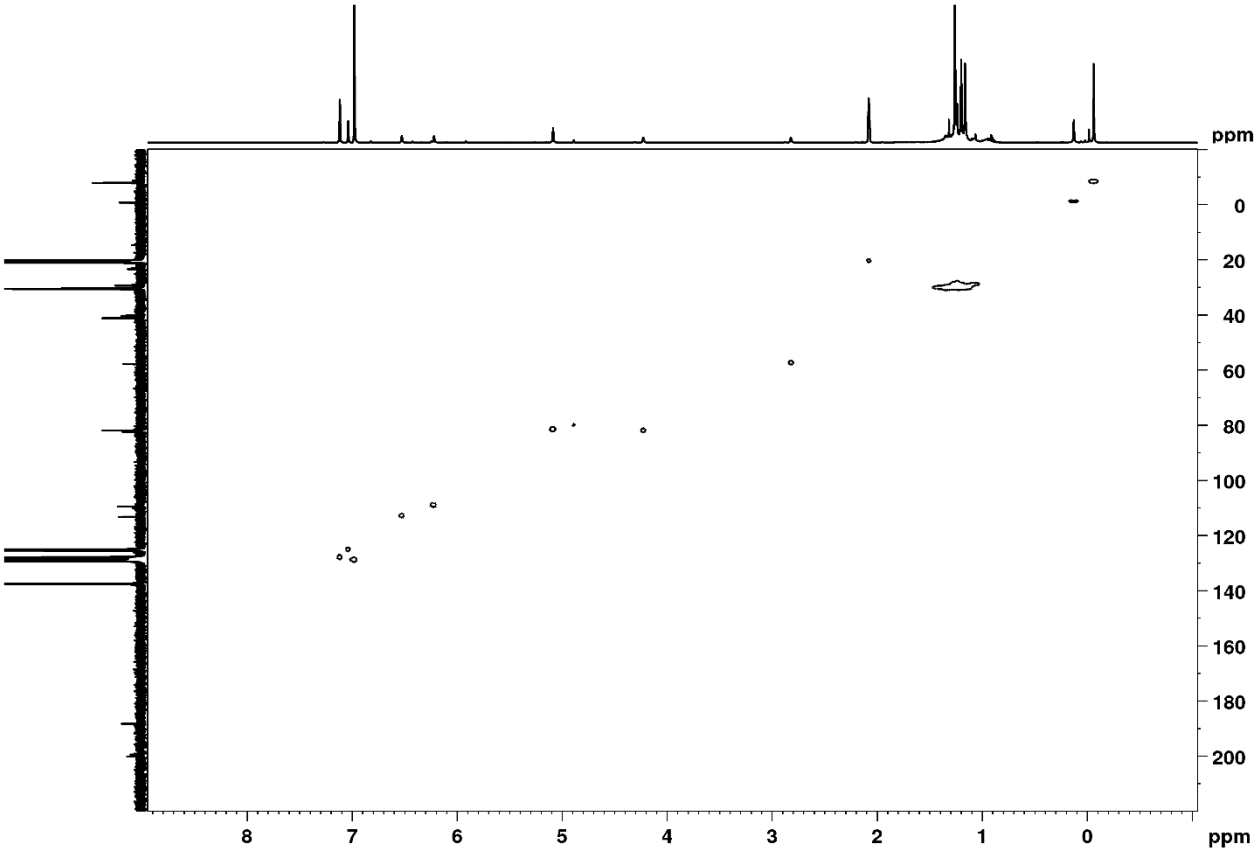

Figure S6. ^{1}H-^{13}C HSQC spectrum (126 MHz) of **5** in toluene-d_8 at –20 °C.

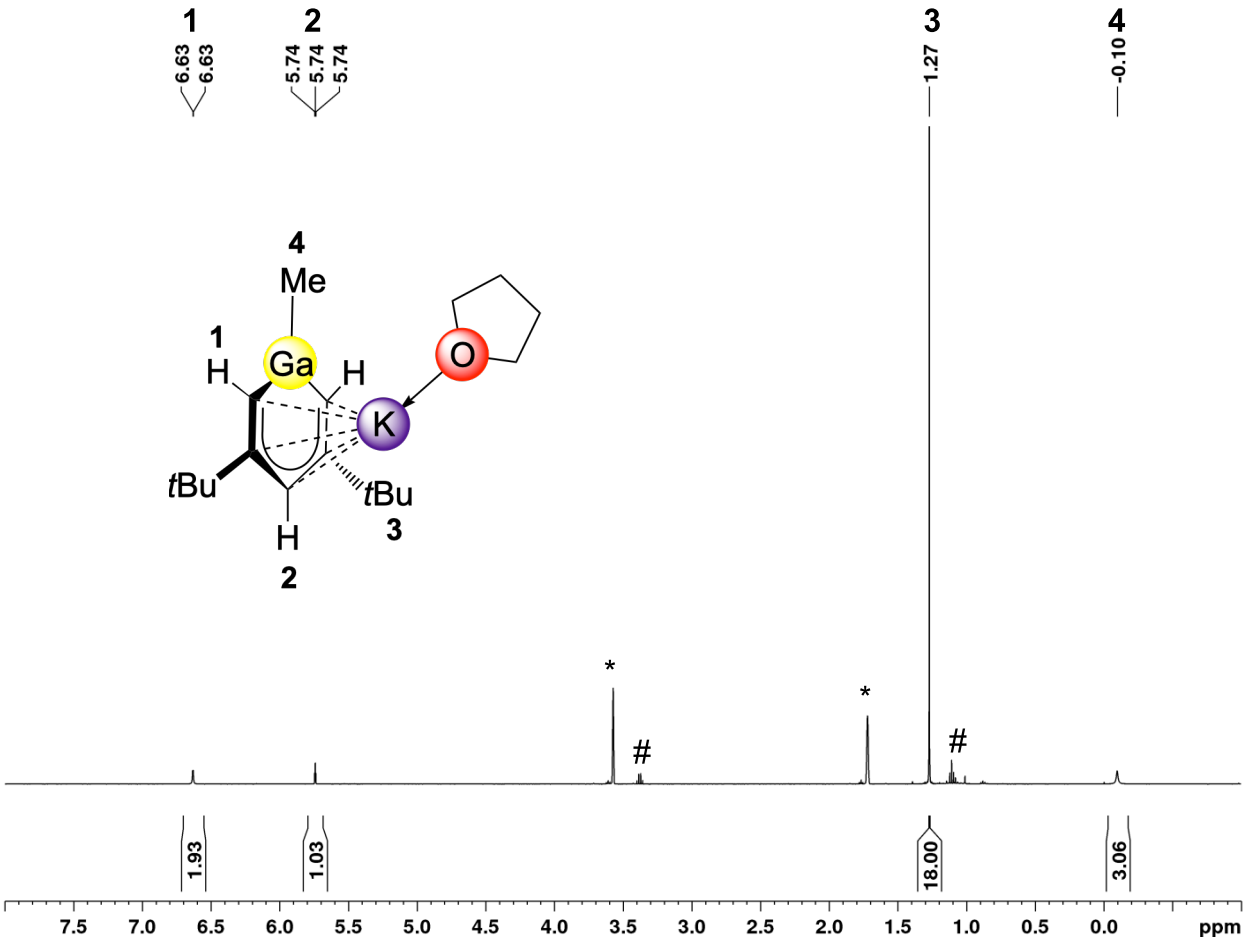

Figure S7. ^{1}H-NMR spectrum (500 MHz) of **6** in thf-d_8 at 26 °C. The solvent residual signal is marked with an asterisk, impurities with #.

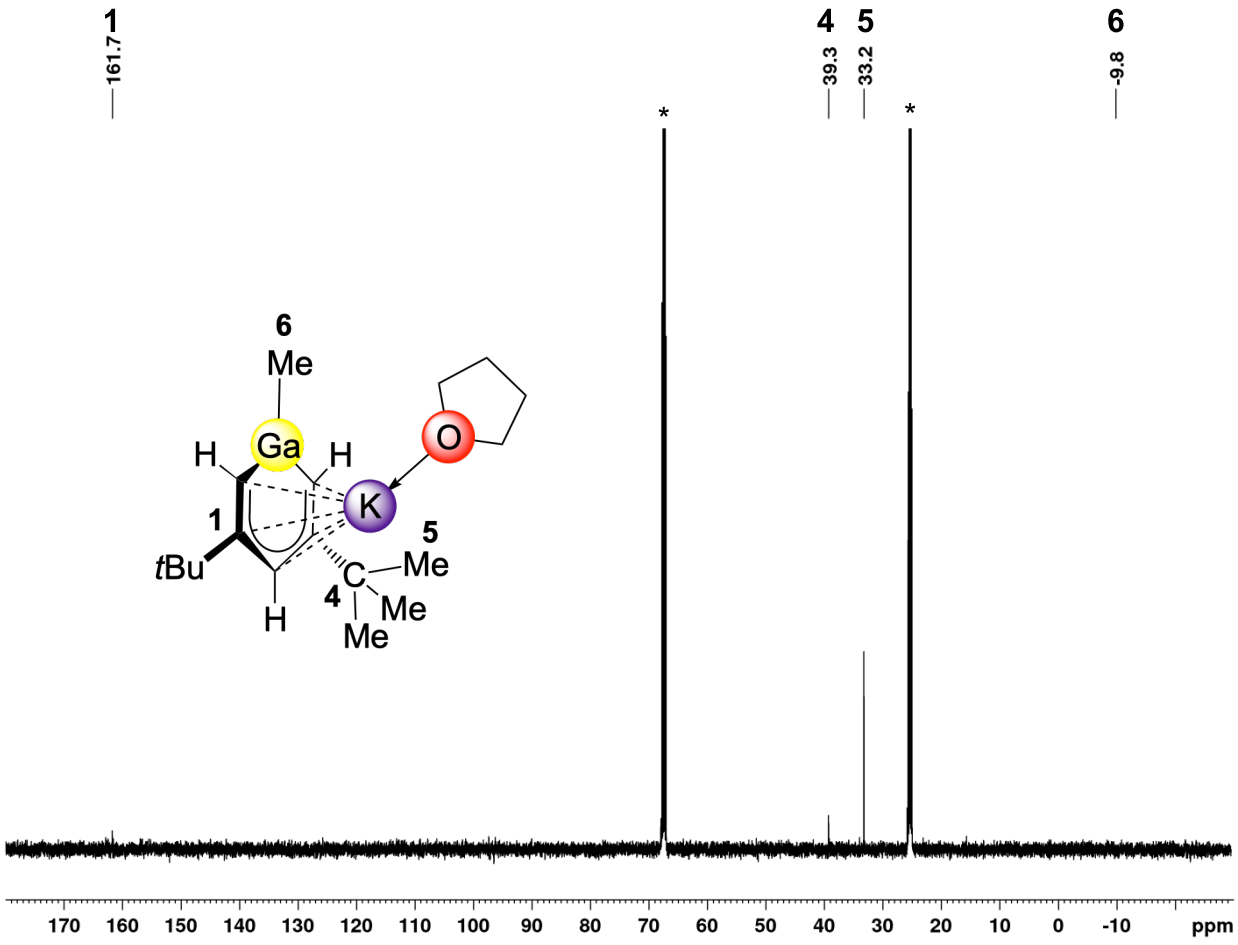

Figure S8. $^{13}C\{^{1}H\}$-NMR spectrum (126 MHz) of **6** in thf-d_8 at 26 °C. The solvent residual signal is marked with an asterisk, impurities with #.

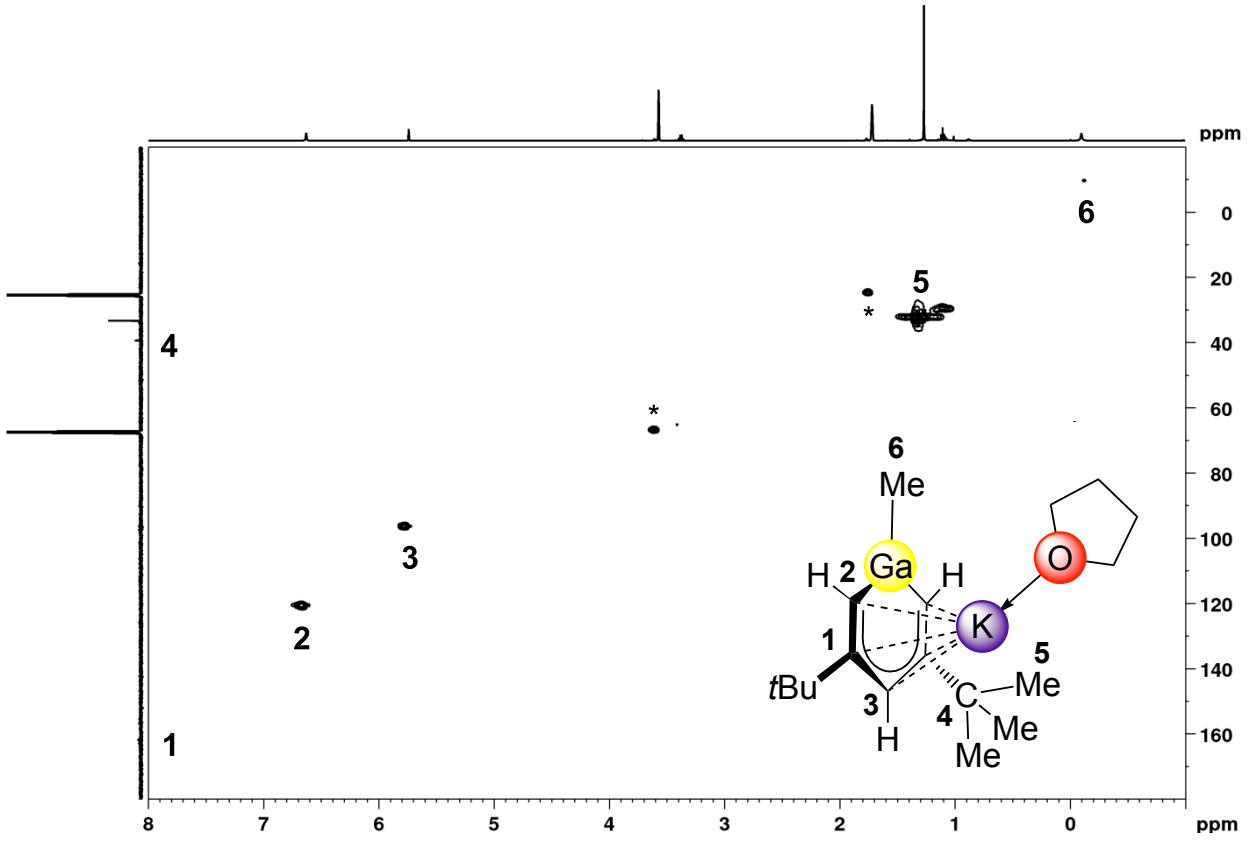

Figure S9. ^{1}H-^{13}C HSQC spectrum (126 MHz) of **6** in thf-d_8 at 26°C.

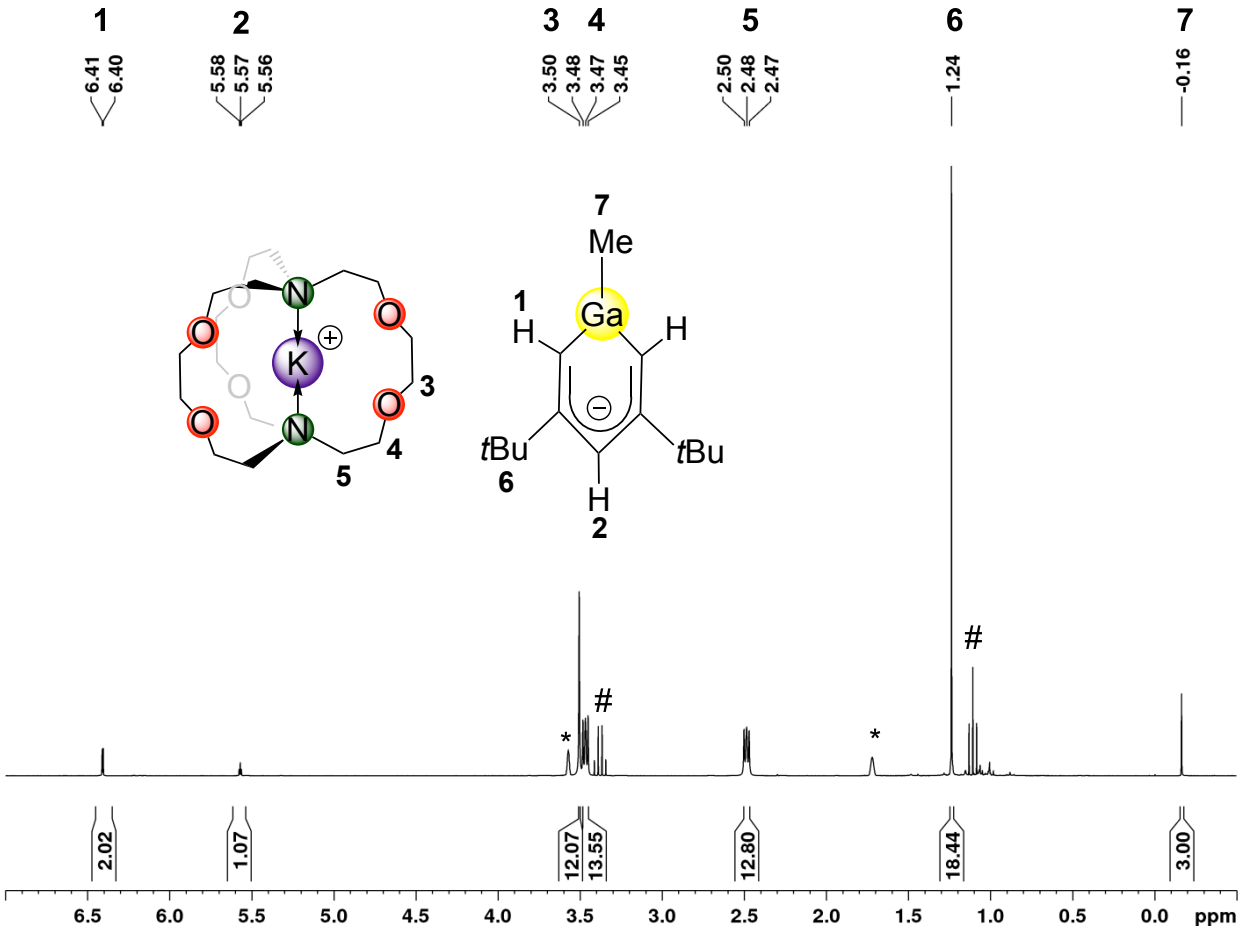

Figure S10. ^{1}H-NMR spectrum (400 MHz) of **7** in thf-d_8 at 26 °C. The solvent residual signal is marked with an asterisk, impurities with #.

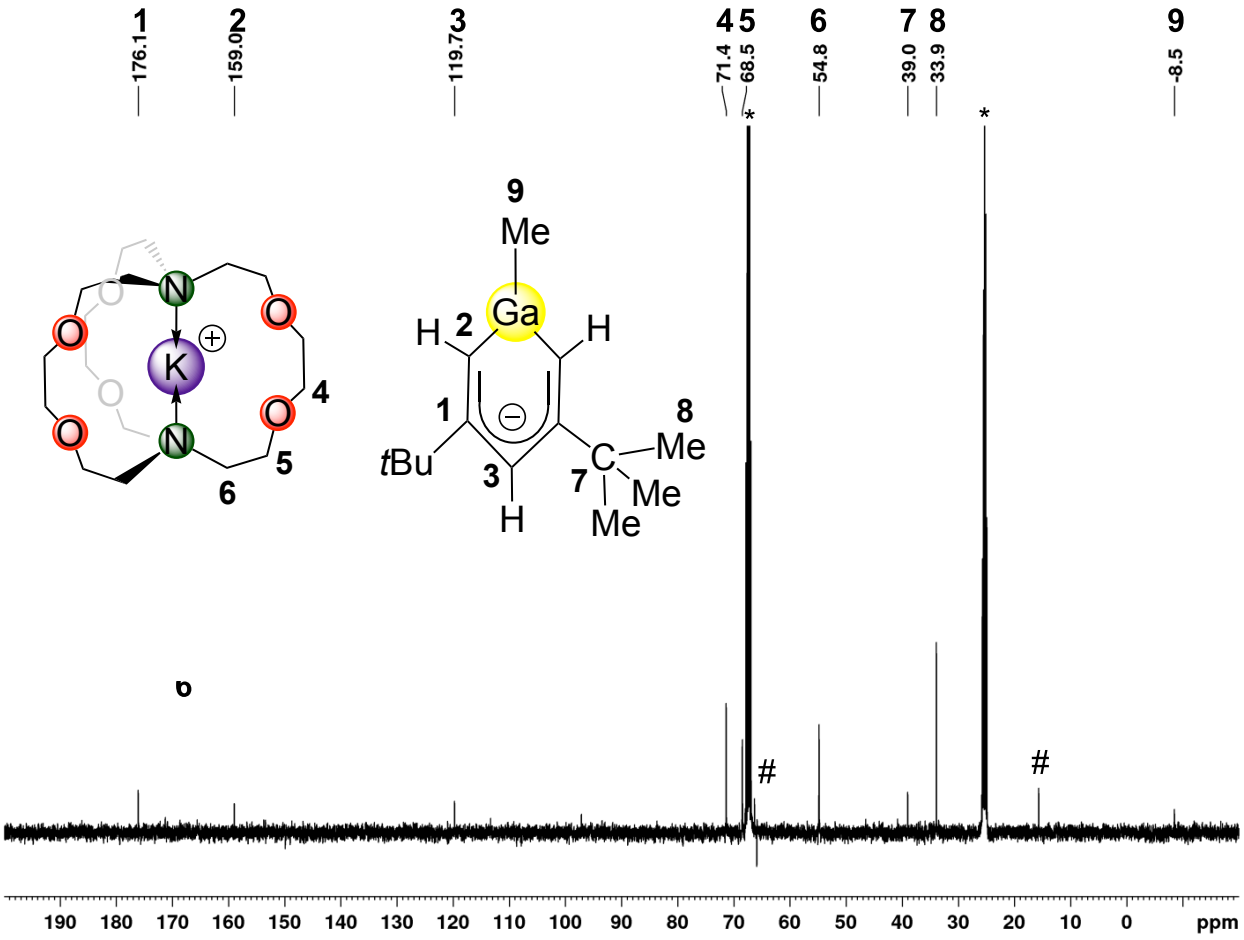

Figure S11. $^{13}C\{^{1}H\}$-NMR spectrum (101 MHz) of **7** in thf-d_8 at 26 °C. The solvent residual signal is marked with an asterisk, impurities with #.

Mass spectrometry (MS)

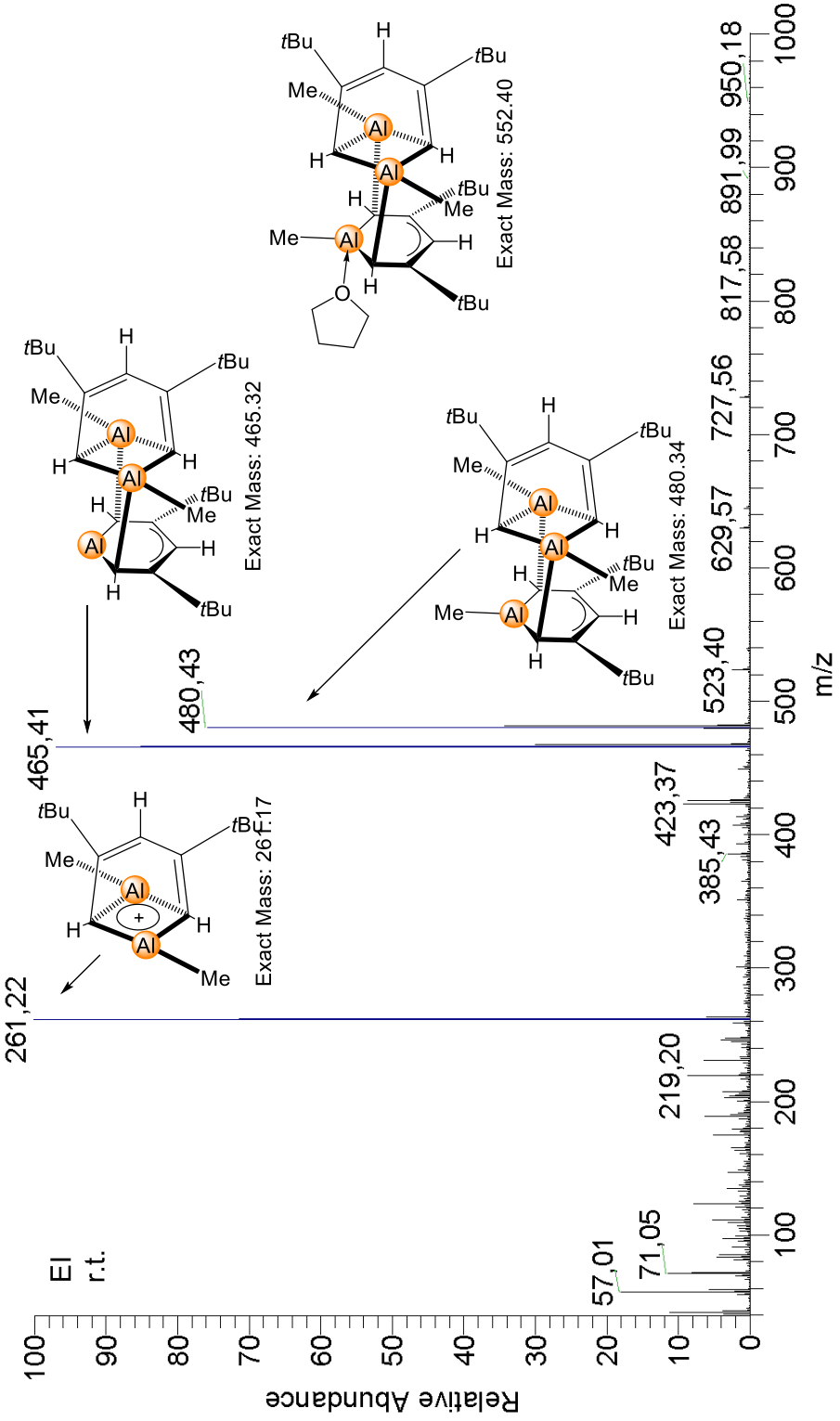

Figure S12. Mass spectrum (EI, 26 °C) of compound **3**.

Crystallography

X-Ray Crystallography and Crystal Structure Determinations. Crystals of **2**–**7** were grown by standard techniques using saturated solutions of *n*-hexane/TMS. Suitable crystals for X-ray structure analyses were selected in a glovebox and coated with Parabar 10312 (previously known as Paratone N, Hampton Research) and fixed on a nylon/loop glass fiber. X-ray data for all compounds were collected on a Bruker APEX II DUO instrument equipped with an IμS microfocus sealed tube and QUAZAR optics for MoK_α (λ = 0.71073 Å) and CuK_α (λ = 1.54184 Å) radiation. The data collection strategy was determined using COSMO[3] employing ω-scans. Raw data were processed using APEX[4] and SAINT,[5] corrections for absorption effects were applied using SADABS[6] and TWINABS[7]. The structures were solved by direct methods and refined against all data by full-matrix least-squares methods on F^2 using SHELXTL[8] and SHELXLE.[9] All graphics were produced employing CCDC Mercury 3.10.1.[10] Further details regarding the refinement and crystallographic data are listed in Table S1 and in the CIF files. CCDC depositions 2491667-2491671 contain all the supplementary crystallographic data for this paper. These data can be obtained free of charge from the Cambridge Crystallographic Data Centre via www.ccdc.cam.ac.uk/data_request/cif.

Table S1. Crystallographic data for compounds **2**, **3**, **5**, **6** and **7**

	2	**3**	**5**	**6**	**7**
CCDC	2491668	2491670	2491669	2491667	2491671
formula	$C_{28}H_{51}Al_2Y$	$C_{33}H_{59}Al_3O$	$C_{29}H_{51}Ga_3$	$C_{18}H_{32}GaKO$	$C_{36}H_{70}N_2O_7GaK$
M_r [g mol^{-1}]	530.55	552.74	608.85	373.25	751.76
color	yellow/plate	orange/rhomb	orange/rhomb	colourless needle	colourless plate
crystal dimensions [mm]	0.204 x 0.133 x 0.084	0.242 x 0.142 x 0.140	0.308 x 0.223 x 0.187	0.440 x 0.126 x 0.064	0.093 x 0.123 x 0.208
crystal system	monoclinic	monoclinic	orthorhombic	monoclinic	monoclinic
space group	$P2_1/c$	$P2_1/c$	$P2_12_12_1$	$P2_1/c$	$P2_1/n$
a [Å]	15.1319(5)	11.711(3)	10.4679(5)	14.941(2)	9.7173(12)
b [Å]	9.5282(3)	17.119(4)	14.1227(7)	12.0009(18)	24.778(3)
c [Å]	20.7917(7)	17.165(4)	20.4969(9)	10.9135(16)	17.120(2)
α [°]	90	90	90	90	90
β [°]	102.0960(10)	90.059(10)	90	92.077(3)	98.452(2)
γ [°]	90	90	90	90	90
V [Å^3]	2931.19(17)	3441.2(14)	3030.2(2)	1955.5(5)	4077.4(9)
Z	4	4	4	4	4
T [K]	100(2)	100(2)	100(2)	100(2)	100(2)
ρ_{calcd} [g·mol^{-3}]	1.202	1.067	1.335	1.268	1.225
μ [mm^{-1}]	2.062	0.132	2.662	1.618	0.822
F (000)	1136	1216	1272	792	1624
θ range [°]	1.376/28.304	1.680/26.358	1.987/ 30.518	1.364/26.387	1.456/26.372
unique reflns	7281	6955	9231	3996	5714
observed reflns	53686	56162	28350	39297	55659
R_1[a]/wR_2 (I>2σ)[b]	0.0310/0.0639	0.0501/0.1086	0.0385/ 0.0790	0.0610/0.1436	0.0422/0.0822
R_1[a]/wR_2 (all data)[b]	0.0497/0.0695	0.0749/0.1222	0.0552/ 0.0851	0.0960/0.1600	0.0783/0.0955
GOF[c]	1.037	1.023	0.984	1.041	1.004

[a] $R_1 = \Sigma(||F_0| - |F_c||) / \Sigma|F_0|$, $F_0 > 4\sigma(F_0)$. [b] $wR_2 = \{\Sigma[w(F_0^2 - F_c^2)^2 / \Sigma[w(F_0^2)^2]\}^{1/2}$. [c] $GOF = [\Sigma w(F_0^2 - F_c^2)^2 / (n_0 - n_p)]^{1/2}$.

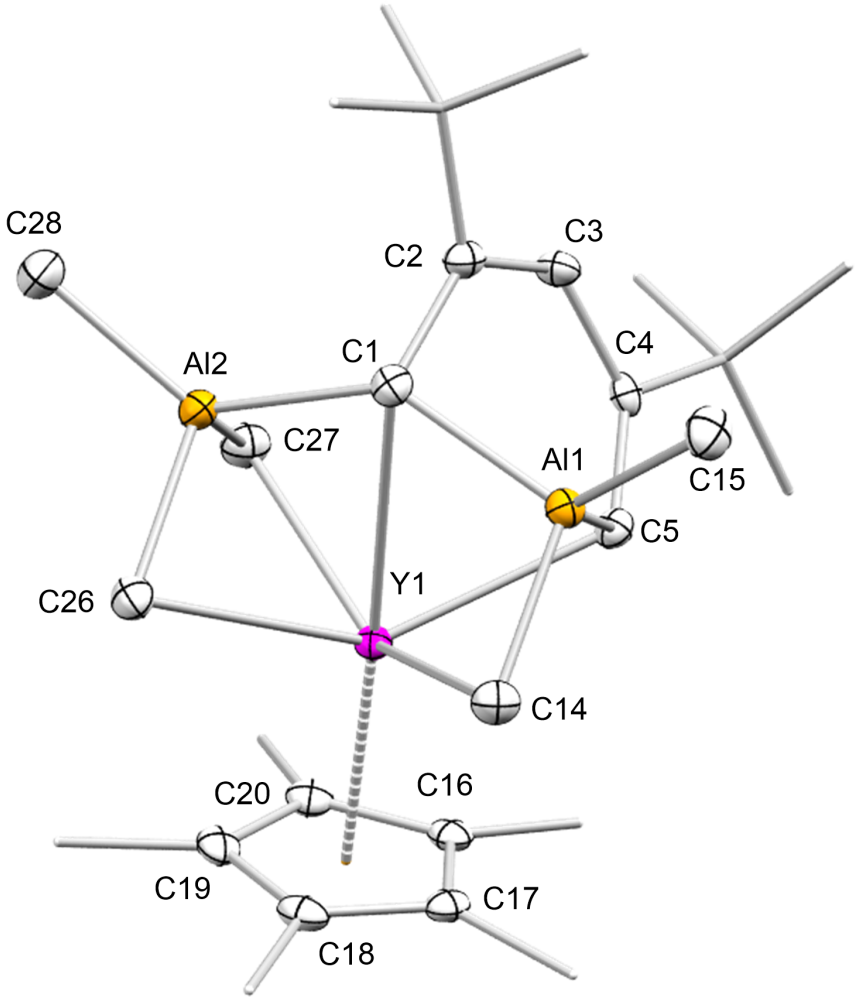

Figure S13. Crystal structure of **2** (ellipsoids set at 50%). All hydrogen atoms have been omitted for clarity. Selected interatomic distances (Å) and angles (°): Y(1)---Al(1) 2.8233(5), Y(1)---Al(2) 2.7999(6), Y(1)–C(1) 2.8095(17), Y(1)–C(5) 2.5144(17), Y(1)–C(14) 2.7281(19), Y(1)–C(26) 2.6928(19), Y(1)–C(16)-C(29) 2.6268(17)-2.6614(17), Al(1)–C(1) 2.0264(18), Al(2)–C(1) 2.0239(18), Al(2)–C(28) 1.9585(19), Al(2)–C(26) 2.048(2), Al(2)–C(27) 2.054(2), Al(1)–C(5) 2.0455(18), Al(1)–C(14) 2.0438(19), Al(1)–C(15) 1.9559(18), C(1)–C(2) 1.484(2), C(2)–C(3) 1.367(2), C(3)–C(4) 1.459(2), C(4)–C(5) 1.379(2); Al(2)-C(1)-Al(1)137.07(9), Al(2)-Y(1)-Al(1) 84.184(16).

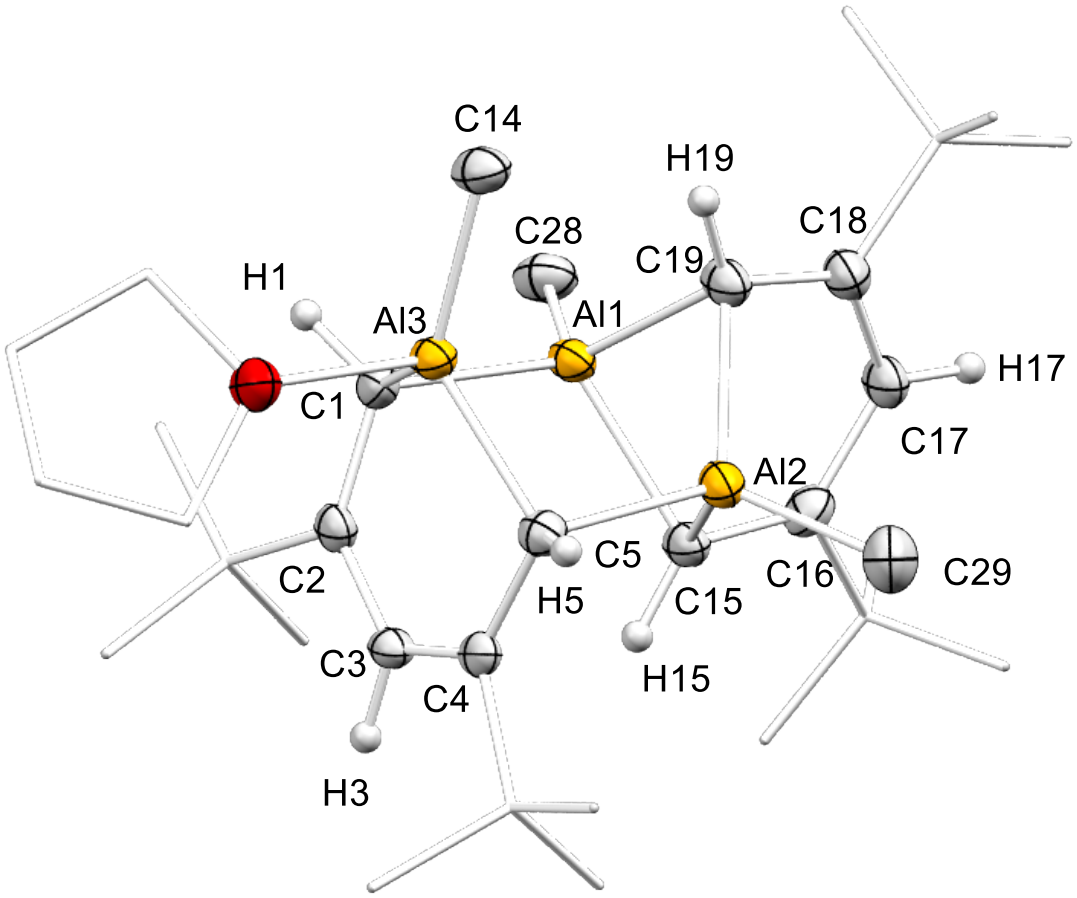

Figure S14. Crystal structure of **3** (ellipsoids set at 50%). Methyl hydrogen atoms have been omitted for clarity. Selected interatomic distances (Å) and angles (°): Al(1)–C(1) 2.072(3), Al(1)---Al(2) 2.6810(14), Al(1)–C(15) 2.040(3), Al(1)–C(19) 2.042(3), Al(1)–C(28) 1.971(3), Al(2)–C(29) 1.971(3), Al(2)–C(19) 2.037(3), Al(2)–C(15) 2.027(3), Al(2)–C(5) 2.071(3), Al(3)–C(1) 1.980(3), Al(3)–C(5) 1.961(3), Al(3)–C(14) 1.968(3), Al(3)–O(1) 1.936(2), C(1)–C(2) 1.421(4), C(2)–C(3) 1.411(4), C(3)–C(4) 1.407(4), C(4)–C(5) 1.428(4), C(15)–C(16) 1.400(4), C(16)–C(17) 1.427(4), C(17)–C(18) 1.389(4), C(18)–C(19) 1.418(4); C(28)–Al(1)–C(15) 114.75(13), C(28)–Al(1)–C(19)–119.92(13), C(15)–Al(1)–C(19) 85.28(12), C(28)–Al(1)–C(1) 110.13(13), C(15)–Al(1)–C(1) 111.03(11), C(19)–Al(1)–C(1) 113.56(12), C(29)–Al(2)–C(15) 118.60(14), C(29)–Al(2)–C(19) 119.00(14), C(15)–Al(2)–C(19) 85.74(12), C(29)–Al(2)–C(5) 108.96(13), C(15)–Al(2)–C(5) 108.23(11), C(19)–Al(2)–C(5) 114.53(11), O(1)–Al(3)–C(5) 106.60(11), O(1)–Al(3)–C(14) 97.72(11), C(5)–Al(3)–C(14) 125.93(13), O(1)–Al(3)–C(1) 102.28(11), C(5)–Al(3)–C(1) 98.37(12), C(14)–Al(3)–C(1) 122.82(13).

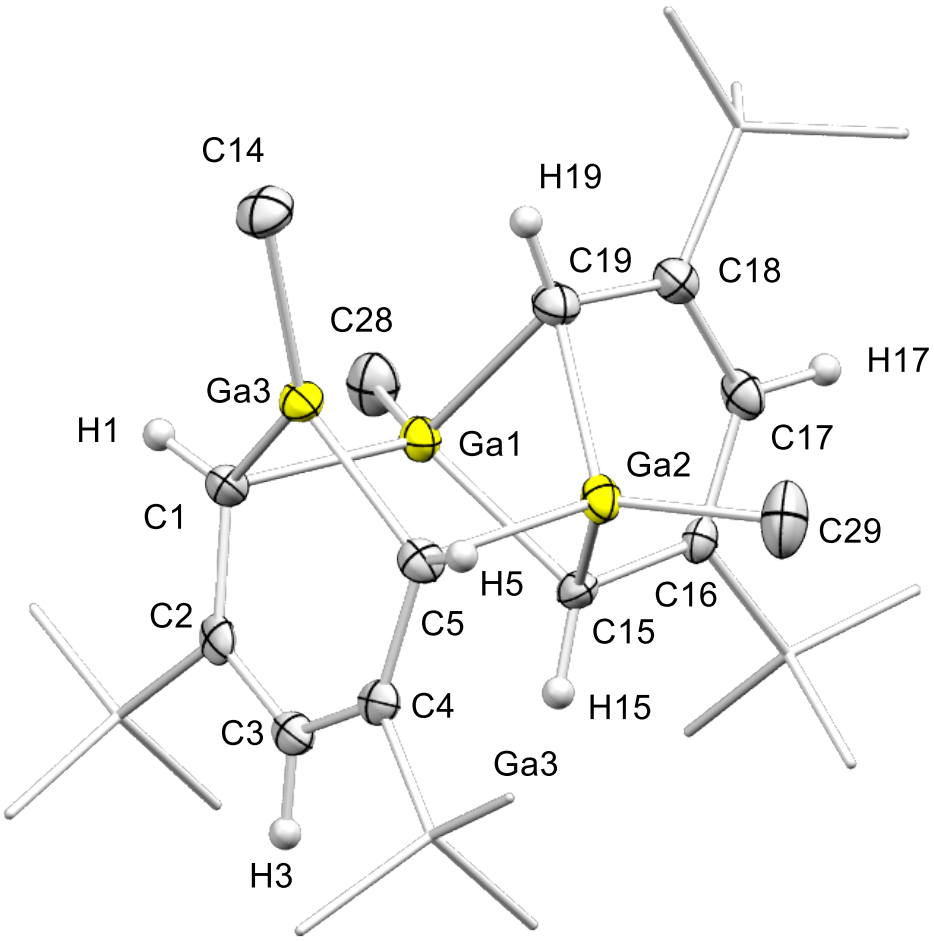

Figure S15. Crystal structure of **5** (ellipsoids set at 50%). Methyl hydrogen atoms have been omitted for clarity. Selected interatomic distances (Å) and angles (°): Ga(1)–C(1) 2.145(4), Ga(1)---Ga(2) 2.8018(6), Ga(1)–C(15) 2.038(4), Ga(1)–C(19) 2.113(4), Ga(1)–C(28) 1.973(4), Ga(2)–C(29) 1.973(4), Ga(2)–C(15) 2.032(4), Ga(2)–C(19) 2.104(4), Ga(2)–C(5) 2.145(4), Ga(3)–C(14) 1.950(4), Ga(3)–C(1) 1.947(4), Ga(3)–C(5) 1.953(4), C(1)–C(2) 1.421(5), C(2)–C(3) 1.395(6), C(3)–C(4) 1.399(6), C(4)–C(5) 1.416(5), C(15)–C(16) 1.432(5), C(16)–C(17) 1.401(5), C(17)–C(18) 1.412(5), C(18)–C(19) 1.412(5); C(28)–Ga(1)–C(15) 119.26(18), C(28)–Ga(1)–C(19) 119.98(18), C(15)–Ga(1)–C(19) 83.38(17), C(28)–Ga(1)–C(1) 110.99(17), C(15)–Ga(1)–C(1) 111.57(15), C(19)–Ga(1)–C(1) 108.86(15); C(29)–Ga(2)–C(15) 120.37(18), C(29)–Ga(2)–C(19) 119.41(19), C(15)–Ga(2)–C(19) 83.73(16), C(29)–Ga(2)–C(5) 110.56(18), C(15)–Ga(2)–C(5) 109.47(15), C(19)–Ga(2)–C(5) 110.68(16), C(1)–Ga(3)–C(14) 130.4(2),C(1)–Ga(3)–C(5) 100.65(16), C(14)–Ga(3)–C(5) 128.9(2).

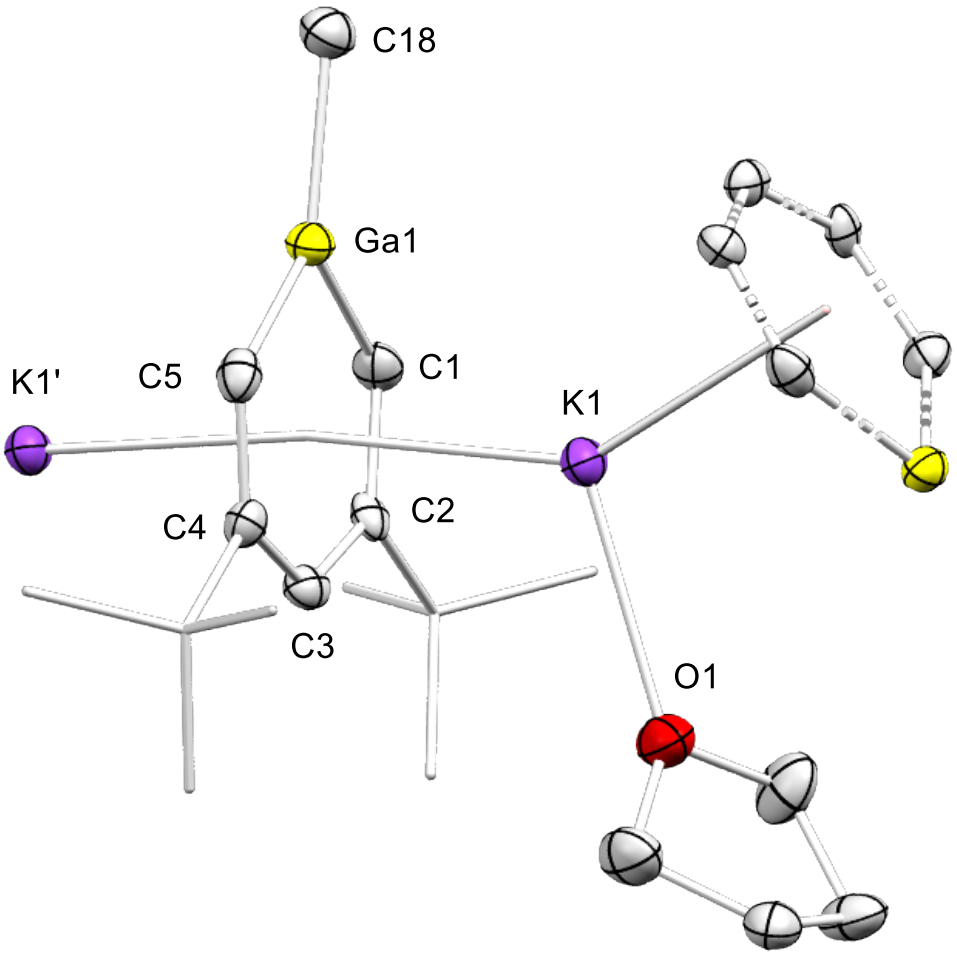

Figure S16. Crystal structure of **6** (ellipsoids set at 50%). All hydrogen atoms have been omitted for clarity. Selected interatomic distances (Å) and angles (°): Ga(1)–C(1) 1.893(5), Ga(1)–C(5) 1.895(5), Ga(1)–C(18) 1.963(5), C(1)–C(2) 1.395(6), C(2)–C(3) 1.424(6), C(3)–C(4) 1.423(6), C(4)–C(5) 1.393(6), K(1)–C(1) 3.295(5), K(1)–C(2) 3.149(4), K(1)–C(3) 3.095(4), K(1)–C(4) 3.188(4), K(1)–C(5) 3.296(5), Ga(1)---K(1) 3.4458(11); C(2)-C(1)-Ga(1) 120.4(3), C(1)-C(2)-C(3) 124.1(4), C(4)-C(3)-C(2) 128.1(4), C(5)-C(4)-C(3) 124.3(4), C(4)-C(5)-Ga(1) 120.4(3).

‘ = x, -y+1/2, z-1/2

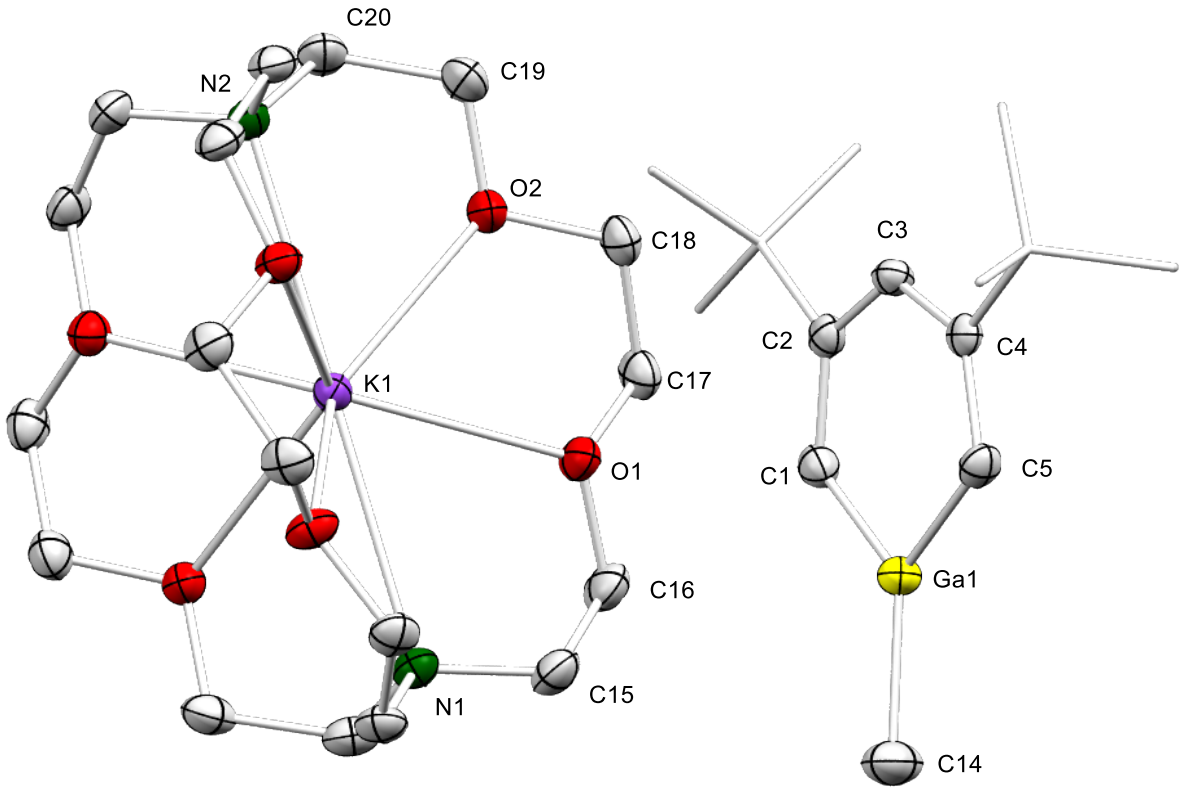

Figure S17. Molecular structure of **7** (ellipsoids set at 50%). All hydrogen atoms and lattice solvent have been omitted for clarity. Selected interatomic distances (Å) and angles (°): Ga(1)–C(1) 1.884(3), Ga(1)–C(5) 1.898(3), Ga(1)–C(14) 1.975(3), C(1)–C(2) 1.395(3), C(2)–C(3) 1.420(4), C(3)–C(4) 1.426(4), C(4)–C(5) 1.386(4); C(1)–Ga(1)–C(5) 104.52(11), C(14)–Ga(1)–C(1) 126.80(12), C(2)–C(1)–Ga(1) 119.15(19), C(4)–C(5)–Ga(1) 118.8(2), C(1)–C(2)–C(3) 124.1(2), C(2)–C(3)–C(4) 128.9(2).

DFT Calculations

Computational Details. DFT calculations were carried out with the Gaussian 16 program package[11] using the B3LYP hybrid functional[12] in combination with the implemented 6-311++G(d,p) basis set for all atoms.[13]

The geometry for the model system [1-Me-3,5-*t*Bu$_2$-C$_5$H$_3$Ga]$^-$, representing the gallatabenzene moiety of **7**, was fully optimized without imposing any symmetry constraints, and also within C_s symmetry, in which the *tert*-butyl substituents were related by mirror symmetry. Both model systems [1-Me-2,6-*t*Bu$_2$-C$_5$H$_3$Ga]$^-$ and [1-Me-3,5-(SiMe$_3$)$_2$-C$_5$H$_3$Ga]$^-$ were also optimized within C_s symmetry, with respect to a plane perpendicular to the heterocyclic ring plane. Model system [1-Mes-2,6-(SiMe$_3$)$_2$-C$_5$H$_3$Ga]$^-$, representing the gallatabenzene moiety of **B**, was optimized within C_s symmetry with respect to the heterocyclic ring plane; a perpendicular mirror plane resulted in an imaginary frequency due to the methyl group in *para* position of the mesityl substituent; for the silyl substituents, all *i*Pr groups were replaced by methyl groups. All structures obtained were confirmed as true minima by calculating analytical frequencies.

The subsequent NBO analyses were carried out using NBO 6.0.[14] All NBO and structural plots were generated using Chemcraft.[15] NICS calculations were performed with Gaussian 16 at the 6-311++G(d,p) level of theory, using the default GIAO method.[11]

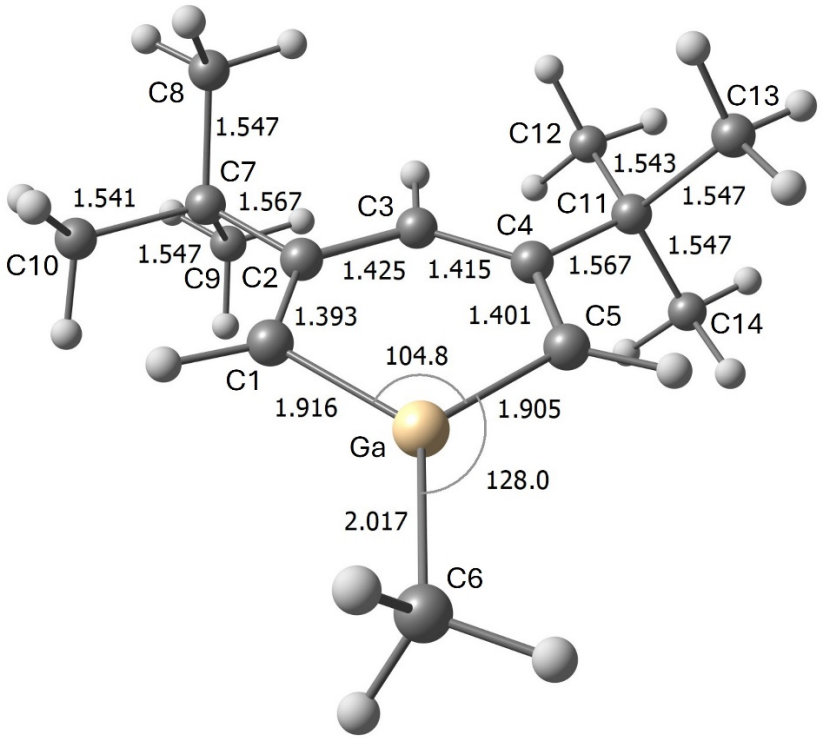

Figure S18. DFT geometry and selected bond parameters for the model system [1-Me-3,5-*t*Bu$_2$-C$_5$H$_3$Ga]$^-$ representing the gallatabenzene moiety of **7**.

Table S2. NPA charges for selected atoms in Figure S18

Atom:	Ga	C1	C2	C3	C4	C5	C6	C7	C11
NPA charge:	+1.18	–0.81	–0.02	–0.37	–0.02	–0.84	–1.11	–0.10	–0.10

Table S3. Hyperconjugative interactions and their NBO energies (in kcal/mol; threshold: 4 kcal/mol) observed for the model system [1-Me-3,5-*t*Bu$_2$-C$_5$H$_3$Ga]$^-$ representing the gallatabenzene moiety of **7**; donor-acceptor interactions describing the delocalized π bonding within the ring are excluded

Donor NBO:	Acceptor NBO:	Energy:
σ(Ga–C1)	σ*(C2–C7)	8.8
σ(Ga–C5)	σ*(C4–C11)	7.6
σ(C1–H)	σ*(C2–C3)	6.5
σ(C5–H)	σ*(C3–C4)	6.5
σ(C3–H)	σ*(C1–C2)	5.7
σ(C3–H)	σ*(C4–C5)	5.7
σ(Ga–C6)	σ*(Ga–C1)	4.9
σ(Ga–C6)	σ*(Ga–C5)	4.9
σ(C11–C12)	σ*(C4–C5)	2.4
σ(C7–C10)	σ*(C2–C3)	2.1

Table S4. Coordinates of the DFT-optimized geometry (in C_1 symmetry) for the model system [1-Me-3,5-*t*Bu$_2$-C$_5$H$_3$Ga]$^-$ representing the gallatabenzene moiety of **7**

6	-1.238259000	-0.441655000	0.000000000
6	0.071691000	-0.976492000	-0.000001000
6	-1.542843000	0.926018000	0.000001000
1	0.139381000	-2.054370000	-0.000002000
1	-2.597775000	1.197982000	0.000003000
6	1.324977000	-0.297297000	0.000000000
6	1.479542000	1.087171000	0.000001000
1	2.491806000	1.479987000	0.000002000
31	-0.101033000	2.170749000	0.000002000
6	-2.443440000	-1.443786000	0.000000000
6	2.577212000	-1.239683000	0.000000000
6	-3.309743000	-1.210607000	-1.259972000
1	-3.675471000	-0.183443000	-1.305995000
1	-2.721437000	-1.391553000	-2.164931000
1	-4.175018000	-1.887156000	-1.270770000
6	-3.309741000	-1.210610000	1.259974000
1	-2.721433000	-1.391558000	2.164931000
1	-3.675468000	-0.183446000	1.305999000
1	-4.175016000	-1.887159000	1.270772000
6	-2.042173000	-2.933198000	-0.000002000
1	-1.456642000	-3.196444000	-0.885219000
1	-1.456641000	-3.196446000	0.885213000
1	-2.945145000	-3.555746000	-0.000002000
6	2.571322000	-2.135874000	-1.261514000
1	2.583493000	-1.518172000	-2.164656000
1	3.453738000	-2.789844000	-1.280329000
1	1.681203000	-2.766079000	-1.306627000
6	2.571321000	-2.135875000	1.261513000
1	3.453737000	-2.789844000	1.280328000
1	2.583490000	-1.518174000	2.164655000
1	1.681201000	-2.766080000	1.306625000
6	3.912396000	-0.471207000	0.000001000
1	4.010941000	0.164683000	-0.883651000
1	4.010940000	0.164682000	0.883653000
1	4.746848000	-1.182895000	0.000001000
6	-0.198929000	4.185240000	-0.000003000
1	-1.236996000	4.533938000	0.000139000
1	0.296265000	4.605538000	0.882377000
1	0.296012000	4.605517000	-0.882536000

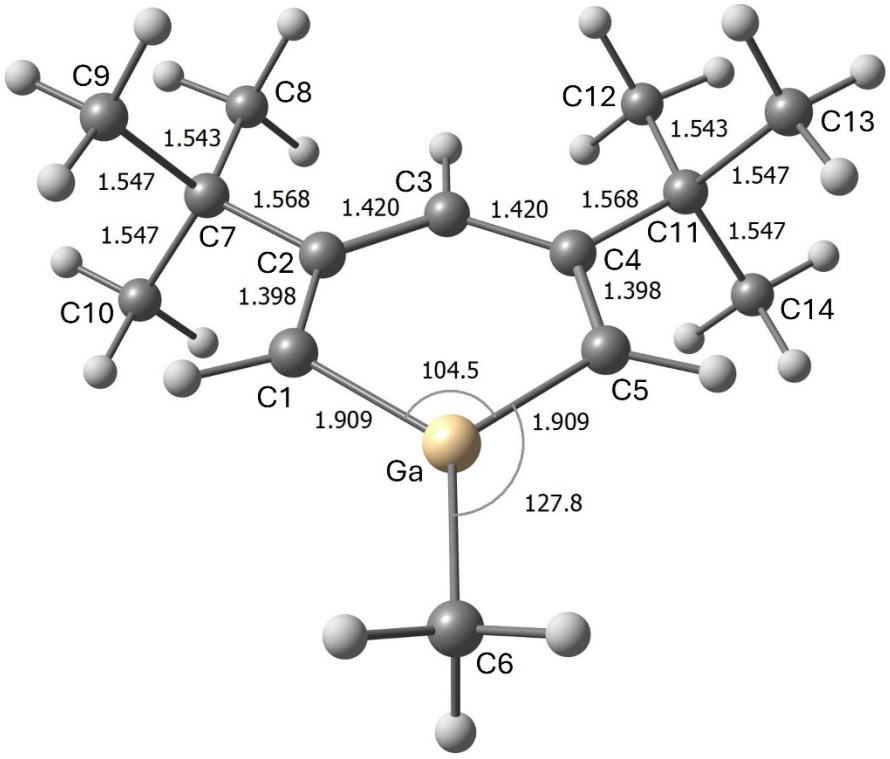

Figure S19. DFT geometry and selected bond parameters for a model system [1-Me-3,5-*t*Bu$_2$-C$_5$H$_3$Ga]$^-$, in which the *tert*-butyl substituents are related by mirror symmetry.

Table S5. NPA charges for selected atoms in Figure S19

Atom:	Ga	C1	C2	C3	C4	C5	C6	C7	C11
NPA charge:	+1.18	–0.82	–0.02	–0.37	–0.02	–0.82	–1.11	–0.10	–0.10

Table S6. Hyperconjugative interactions and their NBO energies (in kcal/mol; threshold: 4 kcal/mol) observed for a model system [1-Me-3,5-*t*Bu$_2$-C$_5$H$_3$Ga]$^-$, in which the *tert*-butyl substituents are related by mirror symmetry; donor-acceptor interactions describing the delocalized π bonding within the ring are excluded

Donor NBO:	Acceptor NBO:	Energy:
σ(Ga–C1)	σ*(C2–C7)	7.6
σ(Ga–C5)	σ*(C4–C11)	7.6
σ(C1–H)	σ*(C2–C3)	6.5
σ(C5–H)	σ*(C3–C4)	6.5
σ(C3–H)	σ*(C1–C2)	5.6
σ(C3–H)	σ*(C4–C5)	5.6
σ(Ga–C6)	σ*(Ga–C1)	4.9
σ(Ga–C6)	σ*(Ga–C5)	4.9

Table S7. Coordinates of the DFT-optimized geometry for a model system [1-Me-3,5-*t*Bu$_2$-C$_5$H$_3$Ga]$^-$, in which the *tert*-butyl substituents are related by mirror symmetry

6	0.399754000	-0.000937000	1.281574000
6	1.011562000	-0.003538000	0.000000000
6	-0.979168000	0.002351000	1.508995000
1	2.087799000	-0.005479000	0.000000000
1	-1.308096000	0.006458000	2.547862000
6	0.399754000	-0.000937000	-1.281574000
6	-0.979168000	0.002351000	-1.508995000
1	-1.308096000	0.006458000	-2.547862000
31	-2.148307000	0.003458000	0.000000000
6	1.334657000	-0.000531000	2.540122000
6	1.334657000	-0.000531000	-2.540122000
6	1.051495000	-1.257732000	3.395556000
1	0.005897000	-1.300232000	3.705414000
1	1.261592000	-2.164639000	2.820073000
1	1.680054000	-1.268264000	4.296307000
6	1.058031000	1.262009000	3.389792000
1	1.272670000	2.165166000	2.810114000
1	0.012691000	1.311234000	3.699547000
1	1.686730000	1.273468000	4.290434000
6	2.843814000	-0.005271000	2.220636000
1	3.136105000	-0.891992000	1.651481000
1	3.141137000	0.877870000	1.648544000
1	3.416126000	-0.005309000	3.156294000
6	2.843814000	-0.005271000	-2.220636000
1	3.136105000	-0.891992000	-1.651481000
1	3.416126000	-0.005309000	-3.156294000
1	3.141137000	0.877870000	-1.648544000
6	1.058031000	1.262009000	-3.389792000
1	1.686730000	1.273468000	-4.290434000
1	0.012691000	1.311234000	-3.699547000
1	1.272670000	2.165166000	-2.810114000
6	1.051495000	-1.257732000	-3.395556000
1	1.261592000	-2.164639000	-2.820073000
1	0.005897000	-1.300232000	-3.705414000
1	1.680054000	-1.268264000	-4.296307000
6	-4.164693000	-0.007392000	0.000000000
1	-4.566636000	0.495291000	0.886141000
1	-4.566636000	0.495291000	-0.886141000
1	-4.551050000	-1.032918000	0.000000000

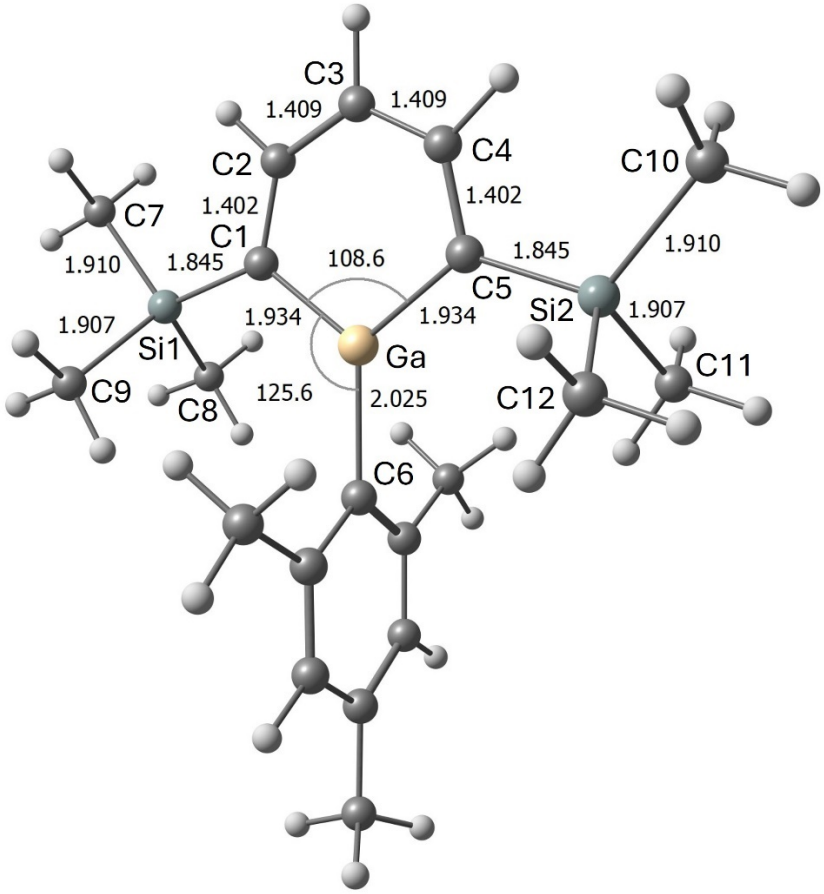

Figure S20. DFT geometry and selected bond parameters for the model system [1-Mes-2,6-$(SiMe_3)_2$-$C_5H_3Ga]^-$ representing the gallatabenzene moiety of **B** (C_s symmetry with respect to the heterocyclic ring plane); for the silyl substituents, *i*Pr groups were replaced by methyl groups.

Table S8. NPA charges for selected atoms in Figure S20

Atom:	Ga	C1	C2	C3	C4	C5	C6	Si1	Si2
NPA charge:	+1.33	–1.14	–0.17	–0.36	–0.18	–1.13	–0.43	+1.63	+1.63

Table S9. Hyperconjugative interactions and their NBO energies (in kcal/mol; threshold: 4 kcal/mol) observed for the model system [1-Mes-2,6-($SiMe_3$)$_2$-C_5H_3Ga]$^-$ representing the gallatabenzene moiety of **B**; donor-acceptor interactions describing the delocalized π bonding within the ring are excluded

Donor NBO:	Acceptor NBO:	Energy:
σ(Ga–C1)	σ*(C2–H)	8.3
σ(Ga–C5)	σ*(C4–H)	8.3
σ(Ga–C6)	σ*(Ga–C1)	6.0
σ(Ga–C6)	σ*(Ga–C5)	6.1
σ(C1–Si1)	σ*(C2–C3)	5.6
σ(C5–Si2)	σ*(C3–C4)	5.5
σ(Ga–C1)	σ*(Ga–C6)	5.0
σ(Ga–C5)	σ*(Ga–C6)	5.2
σ(C2–H)	σ*(Ga–C1)	5.2
σ(C4–H)	σ*(Ga–C5)	5.0
σ(C3–H)	σ*(C1–C2)	4.9
σ(C3–H)	σ*(C4–C5)	5.0
σ(C2–H)	σ*(C3–C4)	4.8
σ(C4–H)	σ*(C1–C2)	4.8
π(C1–C2)	σ*(Si1–C8)	4.0
π(C1–C2)	σ*(Si1–C9)	4.0
π(C4–C5)	σ*(Si2–C11)	4.0
π(C4–C5)	σ*(Si2–C12)	4.0

Table S10. Coordinates of the DFT-optimized geometry (in C_s symmetry) for the model system [1-Mes-2,6-($SiMe_3$)$_2$-C_5H_3Ga]$^-$ representing the gallatabenzene moiety of **B**

6	1.665498000	1.616389000	0.000000000
6	3.040740000	1.344006000	0.000000000
1	3.730874000	2.195688000	0.000000000
6	3.699804000	0.098627000	0.000000000
1	4.787455000	0.127263000	0.000000000
6	3.107123000	-1.179661000	0.000000000
1	3.840950000	-1.994025000	0.000000000
6	1.748061000	-1.523603000	0.000000000
6	-1.445995000	-0.039013000	0.000000000
6	-2.176966000	-0.056925000	1.207749000
6	-3.576698000	-0.092779000	1.194359000
1	-4.116375000	-0.101816000	2.139160000
6	-4.297315000	-0.114140000	0.000000000
6	-3.576698000	-0.092779000	-1.194359000
1	-4.116375000	-0.101816000	-2.139160000
6	-2.176966000	-0.056925000	-1.207749000
6	-1.462282000	-0.033126000	2.543354000
1	-0.788608000	-0.888979000	2.649374000
1	-2.171744000	-0.057760000	3.375717000
1	-0.848122000	0.866284000	2.650538000
6	-5.807014000	-0.190059000	0.000000000
1	-6.155285000	-1.230228000	0.000000000
1	-6.230729000	0.294061000	-0.884728000
1	-6.230729000	0.294061000	0.884728000
6	-1.462282000	-0.033126000	-2.543354000
1	-2.171744000	-0.057760000	-3.375717000
1	-0.788608000	-0.888979000	-2.649374000
1	-0.848122000	0.866284000	-2.650538000

1	0.533236000	3.603980000	-2.446775000
6	-0.024251000	3.762662000	-1.517852000
1	-0.369093000	4.803644000	-1.501768000
1	-0.909298000	3.119460000	-1.547074000
1	0.533236000	3.603980000	2.446775000
6	-0.024251000	3.762662000	1.517852000
1	-0.909298000	3.119460000	1.547074000
1	-0.369093000	4.803644000	1.501768000
1	2.072099000	5.656617000	0.000000000
6	2.475293000	4.637386000	0.000000000
1	3.113554000	4.531298000	-0.883243000
1	3.113554000	4.531298000	0.883243000
1	0.720980000	-3.568187000	2.446758000
6	0.171589000	-3.753768000	1.517988000
1	-0.744310000	-3.155364000	1.548183000
1	-0.120956000	-4.810636000	1.501321000
1	-0.744310000	-3.155364000	-1.548183000
6	0.171589000	-3.753768000	-1.517988000
1	-0.120956000	-4.810636000	-1.501321000
1	0.720980000	-3.568187000	-2.446758000
1	3.344844000	-4.359873000	0.883242000
6	2.712914000	-4.498814000	0.000000000
1	3.344844000	-4.359873000	-0.883242000
1	2.362919000	-5.537515000	0.000000000
14	1.056980000	3.358532000	0.000000000
14	1.230540000	-3.294842000	0.000000000
31	0.578632000	0.016737000	0.000000000

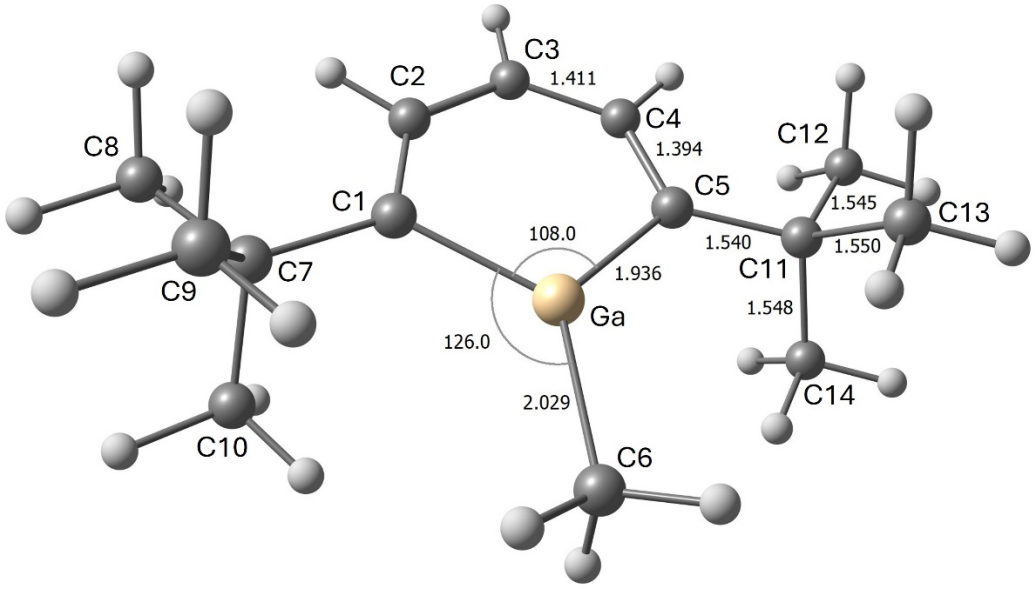

Figure S21. DFT geometry and selected bond parameters for the model system [1-Me-2,6-*t*Bu$_2$-C$_5$H$_3$Ga]$^-$ (C_s symmetry with regards to a plane perpendicular to the heterocyclic ring plane).

Table S9. NPA charges for selected atoms in Figure S21

Atom:	Ga	C1	C2	C3	C4	C5	C6	C7	C11
NPA charge:	+1.22	–0.59	–0.22	–0.36	–0.22	–0.59	–1.14	–0.12	–0.12

Table S10. Hyperconjugative interactions and their NBO energies (in kcal/mol; threshold: 4 kcal/mol) observed for the model system [1-Me-2,6-*t*Bu$_2$-C$_5$H$_3$Ga]$^-$, donor-acceptor interactions describing the delocalized π bonding within the ring are excluded

Donor NBO:	Acceptor NBO:	Energy:
σ(Ga–C1)	σ*(C2–H)	8.1
σ(Ga–C5)	σ*(C4–H)	8.1
σ(Ga–C6)	σ*(Ga–C1)	5.7
σ(Ga–C6)	σ*(Ga–C5)	5.7
σ(C3–H)	σ*(C1–C2)	5.1
σ(C3–H)	σ*(C4–C5)	5.1
σ(C2–H)	σ*(C3–C4)	4.7
σ(C4–H)	σ*(C1–C2)	4.7
σ(Ga–C1)	σ*(Ga–C6)	4.5
σ(Ga–C5)	σ*(Ga–C6)	4.5
σ(C2–H)	σ*(Ga–C1)	4.5
σ(C4–H)	σ*(Ga–C5)	4.5

Table S11. Coordinates of the DFT-optimized geometry (in C_s symmetry) for the model system [1-Me-2,6-*t*Bu$_2$-C$_5$H$_3$Ga]$^-$

6	-1.893103000	0.016825000	1.266025000
6	-2.516659000	0.020018000	0.000000000
6	-0.532048000	0.011213000	1.566346000
1	-3.604646000	0.029002000	0.000000000
6	-1.893103000	0.016825000	-1.266025000
6	-0.532048000	0.011213000	-1.566346000
31	0.605431000	0.004354000	0.000000000
6	2.633981000	0.022103000	0.000000000
1	3.045778000	-0.475617000	0.884117000
1	3.045778000	-0.475617000	-0.884117000
1	3.012296000	1.051220000	0.000000000
1	-2.606180000	0.021273000	2.094558000
1	-2.606180000	0.021273000	-2.094558000
6	-0.038342000	-0.005829000	-3.024823000
6	-0.038342000	-0.005829000	3.024823000
6	0.720560000	-1.327235000	3.306157000
1	1.114168000	-1.355408000	4.332673000
1	0.054302000	-2.183868000	3.167889000
1	1.559063000	-1.447338000	2.615784000
6	-1.163774000	0.111152000	4.076207000
1	-1.735265000	1.035587000	3.949147000
1	-1.864174000	-0.726967000	4.013922000
1	-0.736720000	0.114524000	5.086590000
6	0.937517000	1.172144000	3.264361000
1	0.428219000	2.126409000	3.099586000
1	1.333383000	1.162818000	4.290044000
1	1.782593000	1.125005000	2.573443000
6	0.720560000	-1.327235000	-3.306157000
1	1.114168000	-1.355408000	-4.332673000
1	1.559063000	-1.447338000	-2.615784000
1	0.054302000	-2.183868000	-3.167889000
6	0.937517000	1.172144000	-3.264361000
1	0.428219000	2.126409000	-3.099586000
1	1.782593000	1.125005000	-2.573443000
1	1.333383000	1.162818000	-4.290044000
6	-1.163774000	0.111152000	-4.076207000
1	-1.735265000	1.035587000	-3.949147000
1	-0.736720000	0.114524000	-5.086590000
1	-1.864174000	-0.726967000	-4.013922000

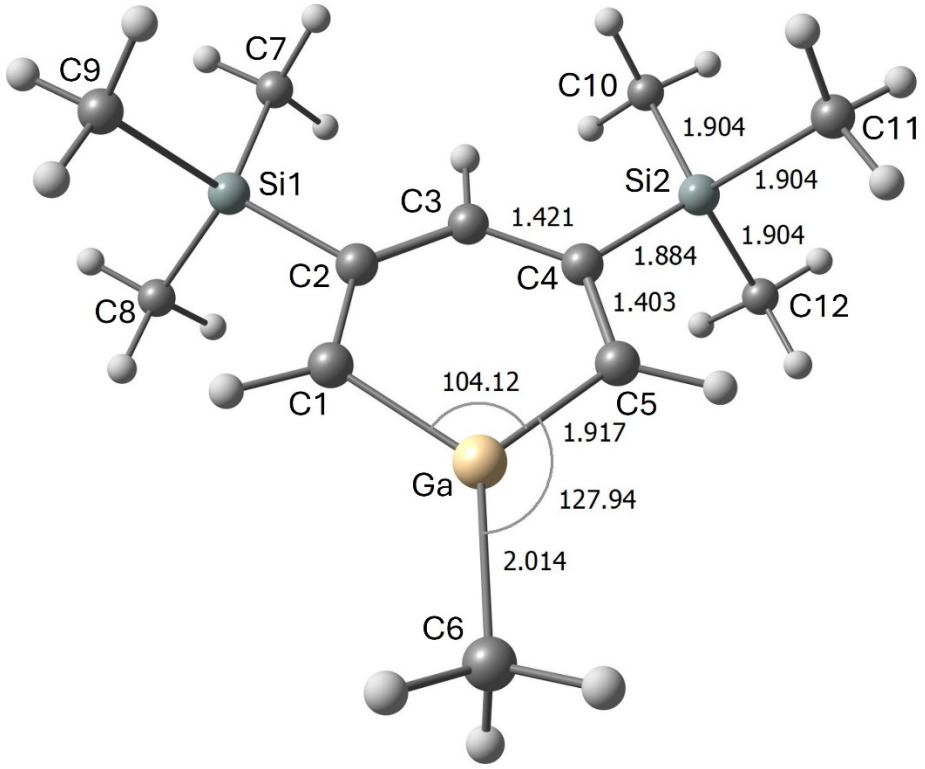

Figure S22. DFT geometry and selected bond parameters for a model system [1-Me-3,5-$(SiMe_3)_2$-$C_5H_3Ga]^-$, in which the silyl substituents are related by mirror symmetry.

Table S12. NPA charges for selected atoms in Figure S22

Atom:	Ga	C1	C2	C3	C4	C5	C6	Si1	Si2
NPA charge:	+1.17	−0.78	−0.50	−0.30	−0.50	−0.78	−1.11	+1.61	+1.61

Table S13. Hyperconjugative interactions and their NBO energies (in kcal/mol; threshold: 4 kcal/mol) observed for the model system [1-Me-3,5-$(SiMe_3)_2$-$C_5H_3Ga]^-$; donor-acceptor interactions describing the delocalized π bonding within the ring are excluded

Donor NBO:	Acceptor NBO:	Energy:
σ(Ga–C1)	σ*(C2–Si1)	5.1
σ(Ga–C5)	σ*(C4–Si2)	5.1
σ(C1–H)	σ*(C2–C3)	5.8
σ(C5–H)	σ*(C3–C4)	5.8
σ(C3–H)	σ*(C1–C2)	5.6
σ(C3–H)	σ*(C4–C5)	5.6
σ(Ga–C6)	σ*(Ga–C1)	4.9
σ(Ga–C6)	σ*(Ga–C5)	4.9
σ(C2–Si1)	σ*(C3–C4)	4.9
σ(C2–Si1)	σ*(Ga–C1)	4.8
σ(C4–Si2)	σ*(C2–C3)	4.9
σ(C4–Si2)	σ*(Ga–C5)	4.8

Table S14. Coordinates of the DFT-optimized geometry (in C_s symmetry) for the model system [1-Me-3,5-$(SiMe_3)_2$-C_5H_3Ga]$^-$

6	-0.149000000	0.001257000	1.276860000
6	-0.772171000	0.004341000	0.000000000
6	1.234610000	-0.002434000	1.511900000
1	-1.858760000	0.006790000	0.000000000
1	1.555966000	-0.007042000	2.556846000
6	-0.149000000	0.001257000	-1.276860000
6	1.234610000	-0.002434000	-1.511900000
1	1.555966000	-0.007042000	-2.556846000
31	2.413379000	-0.003562000	0.000000000
14	-1.250070000	0.000393000	2.806048000
14	-1.250070000	0.000393000	-2.806048000
6	-0.914228000	1.528083000	3.890836000
1	0.142751000	1.582238000	4.167845000
1	-1.155736000	2.446245000	3.345726000
1	-1.508398000	1.511540000	4.812173000
6	-0.920278000	-1.532863000	3.884789000
1	-1.165064000	-2.447923000	3.335949000
1	0.136398000	-1.592099000	4.161898000
1	-1.514655000	-1.517725000	4.806013000
6	-3.112690000	0.004979000	2.411025000
1	-3.398162000	0.889461000	1.833404000
1	-3.401922000	-0.876330000	1.830443000
1	-3.700485000	0.004690000	3.336360000
6	-3.112690000	0.004979000	-2.411025000
1	-3.398162000	0.889461000	-1.833404000
1	-3.700485000	0.004690000	-3.336360000
1	-3.401922000	-0.876330000	-1.830443000
6	-0.920278000	-1.532863000	-3.884789000
1	-1.514655000	-1.517725000	-4.806013000
1	0.136398000	-1.592099000	-4.161898000
1	-1.165064000	-2.447923000	-3.335949000
6	-0.914228000	1.528083000	-3.890836000
1	-1.155736000	2.446245000	-3.345726000
1	0.142751000	1.582238000	-4.167845000
1	-1.508398000	1.511540000	-4.812173000
6	4.427708000	0.007778000	0.000000000
1	4.829365000	-0.494246000	0.886334000
1	4.829365000	-0.494246000	-0.886334000
1	4.811668000	1.034017000	0.000000000

References

1 J. Lebon, D. Barisic, C. Maichle-Mössmer and R. Anwander, *Chem. Eur. J.*, 2023, **29**, e202302846.

2 J. Lebon, M. Beauvois, C. Maichle-Mössmer, P. Sirsch and R. Anwander, *Chem. Eur. J.*, 2024, **30**, e202403472.

3 COSMO, v. 1.61; Bruker AXS Inc., Madison, WI 2012.

4 APEX3 V. 2019.11-0, Bruker AXS Inc., Madison, WI, 2019.

5 SAINT V. 8.40B, Bruker Nano, Inc., Madison, WI, 2019.

6 SADABS. L. Krause, R. Herbst-Irmer, , G. M. Sheldrick & D. Stalke, *J. Appl. Cryst.*, 2015, **48**, 3-10.

7 G. M. Sheldrick, *TWINABS*. University of Göttingen, Germany, 2009.

8 G. M. Sheldrick, *Acta Crystallogr. C Struct. Chem.*, 2015, **71**, 3-8.

9 C. B. Hubschle, G. M. Sheldrick and B. Dittrich, *J. Appl. Crystallogr.*, 2011, **44**, 1281-1284.

10 C. F. Macrae, I. J. Bruno, J. A. Chisholm, P. R. Edgington, P. McCabe, E. Pidcock, L. Rodriguez-Monge, R. Taylor, J. van de Streek and P. A. Wood, *J. Appl. Crystallogr.*, 2008, **41**, 466-470.

11 Gaussian 16, Revision C.01, M. J. Frisch, G. W. Trucks, H. B. Schlegel, G. E. Scuseria, M. A. Robb, J. R. Cheeseman, G. Scalmani, V. Barone, G. A. Petersson, H. Nakatsuji, X. Li, M. Caricato, A. V. Marenich, J. Bloino, B. G. Janesko, R. Gomperts, B. Mennucci, H. P. Hratchian, J. V. Ortiz, A. F. Izmaylov, J. L. Sonnenberg, D. Williams-Young, F. Ding, F. Lipparini, F. Egidi, J. Goings, B. Peng, A. Petrone, T. Henderson, D. Ranasinghe, V. G. Zakrzewski, J. Gao, N. Rega, G. Zheng, W. Liang, M. Hada, M. Ehara, K. Toyota, R. Fukuda, J. Hasegawa, M. Ishida, T. Nakajima, Y. Honda, O. Kitao, H. Nakai, T. Vreven, K. Throssell, J. A. Montgomery, Jr., J. E. Peralta, F. Ogliaro, M. J. Bearpark, J. J. Heyd, E. N. Brothers, K. N. Kudin, V. N. Staroverov, T. A. Keith, R. Kobayashi, J. Normand, K. Raghavachari, A. P. Rendell, J. C. Burant, S. S. Iyengar, J. Tomasi, M. Cossi, J. M. Millam, M. Klene, C. Adamo, R. Cammi, J. W. Ochterski, R. L. Martin, K. Morokuma, O. Farkas, J. B. Foresman and D. J. Fox, Gaussian, Inc., Wallingford CT, 2019.

12 a) A. D. Becke, *J. Chem. Phys.*, 1993, **98**, 5648-5652; b) C. Lee, W. Yang, R. G. Parr, *Phys. Rev. B*, 1988, **37***,* 785-789.

13 a) A. D. McLean and G. S. Chandler, *J. Chem. Phys.*, 1980, **72**, 5639-5648; b) K. Raghavachari, J. S. Binkley, R. Seeger and J. A. Pople, *J. Chem. Phys.*, 1980, **72**, 650-654.

14 NBO 6.0, E.D. Glendening, J. K. Badenhoop, A. E. Reed, J. E. Carpenter, J. A. Bohmann, C. M. Morales, C. R. Landis and F. Weinhold, Theoretical Chemistry Institute, University of Wisconsin, Madison, WI, 2013.

15 G. A. Zhurko, CHEMCRAFT (http://www.chemcraftprog.com).